A comparative study of available water in the major river basins of the world

Venkat Lakshmi* and Jessica Fayne
School of Earth Ocean and the Environment, University of South Carolina, Columbia SC 29208 USA, vlakshmi@geol.sc.edu
*Corresponding author

John Bolten
NASA Goddard Space Flight Center, Greenbelt MD 20771 USA

Revised and Submitted to *Journal of Hydrology*

September 2018

Abstract

Numerous large river basins of the world have few and irregular observations of the components of the terrestrial hydrological cycle with the exception of stream gauges at a few locations and at the outlet along with sparsely distributed rain gauges. Using observations from satellite sensors and output from global land surface models, it is possible to study these under-observed river basins. With populations greater than a billion people, some of these rivers (e.g., the Ganga-Brahmaputra, the Yangtze, the Nile and the Mekong) are the economic engines of the countries they transect, yet thorough assessment of their flow dynamics and variability in regard to water resource management is still lacking. In this paper, we use soil moisture (0-2m) and surface runoff from the NASA Global Land Data Assimilation System (GLDAS), evapotranspiration, and Normalized Difference Vegetation Index (NDVI) from the Moderate Resolution Imaging Spectroradiometer (MODIS) and rainfall from the Tropical Rainfall Measuring Mission (TRMM) and total water storage anomaly from the Gravity Recovery and Climate Experiment (GRACE) to examine variability of individual water balance components. To this end, understanding the inter-annual and intra-seasonal variability and the spatial variability of the water balance components in the major river basins of the world will help to plan for improved management of water resources for the future.

1.0 Introduction

The water availability per capita in many locations of the world is constantly decreasing. One explanation is the increasing proportion of global population relative to the available water in many parts of the world. The global population has increased from 2 billion in 1950 to a current population of 7.4 billion - for essentially the same water availability, the global per capita water availability has an inverse relationship, decreasing by a factor greater than 3 during this period. However, there are two reasons that this conclusion is not global. Firstly, the distribution of population increase is not uniform - for example: urban growth is significantly different in areas in Asia and Africa as compared to Europe and Australia and secondly, in many regions of the world, the groundwater is a predominant source of water and is being exploited and it has only recently become obvious that withdrawal rates from these aquifers are unsustainable. For example, groundwater in the High Plains of the United States and in Northern India are over utilized.

The United Nations World Water Development Report 2016 points out that three out of four jobs globally are dependent on water (UN Water, 2016). There are numerous areas such as agriculture, power production, industrial applications, fishing and health, which involve water - illustrating the societal dependence on water.

Numerous studies have pointed out the impacts of climate change and/or population growth on water resources (Arnell, 1999, Alcamo et al. 2007, Kundzewicz, Z.W., et al 2007, Oki and Kanae, 2006, Piao et al. 2010, Ragab and Prudhomme, 2002, Vorosmarty et al. 2000). Other studies have addressed more specific changes such as groundwater recharge under various climate change scenarios (Herrera-Pantoja and Hiscock, 2008, Scanlon et al. 2006, Taylor et al. 2013). One common conclusion from all these studies is that the amount of water available is decreasing with both climate change and increasing population.

The major river basins of the world play a big role in supporting over 70% of the global population. Many of these hydrological studies are specific to a river basin but there are a few

comparative studies across river basins (Aerts et al. 2006, Dai et al. 2009, Nijssen et al. 2001, Oki and Kanae, 2006, Vorosmarty et al. 2000). In their study of global rivers using various climate models under different scenarios of climate change Nijssen et al. 2001 found that the largest changes were observed in the spring time period that corresponds to the snowmelt. Aerts et al. 2006 found that the future discharges in some of the major river basins could increase by 6-16% due to changes in climate. The analysis of the annual stream flows for the 200 largest rivers of the world from 1948-2004 showed that more rivers exhibited decreasing trends than increasing trends (Dai et al. 2009). Vorosmarty et al. 2000 and Oki and Kanae 2006 both showed that the water scarcity index showed higher values in Western United States, Northern Africa, South Asia and the Middle East regions and that the population living in the area of high water stress and relative demand for water would increase with the changes in climate.

Observations of the water cycle using in-situ sensors are very difficult due to two reasons. Firstly, the water cycle is highly heterogeneous in space and varies temporally at short time scales. Maintenance and operation of a high-density in-situ network (for example rain gauges) is very expensive. Secondly, obtaining data from river basins in countries other than United States is at times very difficult since many countries may not freely distribute or share data. Given these reasons, satellite remote sensing observations and hydrological model outputs are an attractive solution that can overcome spatial heterogeneity and temporal consistency issues. In addition, the quasi-global coverage provided by satellite observations combined with open data policies can help avoid the issues related to data access and continuity.

The motivation of this study is two-fold. Firstly, the lack of in-situ water data from most of the large river basins of the world implies that we can only use the readily available satellite data sets and global land model outputs. Secondly, most of the studies that involved these major river basins were published at least a decade or so ago and current up to-date studies do not exist. We currently have about 15 years of data from satellite sensors that can bridge this gap. In this work, we mostly use satellite data from NASA satellite sensors as they have long data records (over 10

years in all cases) and are freely and publicly available. The model outputs also come from a NASA model system, the Global Land Data Assimilation System, which is also publicly available.

Here, we use publicly available data sets to construct the water balance of eleven large continental scale river basins of the world. We analyze each of the components of the water budget (precipitation, evapotranspiration runoff and total water) for seasonality and study the spatial and temporal correlations between components. In this way, we envisage that this study will help water resource managers with future planning of water resources and land use in these highly important and widely utilized river basins.

This paper is organized as follows – section 2 describes the data sets – satellite and model derived for the variables in the hydrological cycle; section 3 highlights the results for the hydrological cycle for the major river basins using the data described in section 2 and identify key processes in time and space. Finally, section 4 delves into the conclusions and discussions of this work.

2.0 Data

All the data sets used in this study are the monthly averaged or cumulative (precipitation) values and at their inherent spatial resolution. All of the data sources are listed in Table 1. Time series are calculated from the spatial average within the respective basins; no attempt has been made to re-grid the data to a common spatial resolution in the figures, tables and analyses in this paper.

2.1 TRMM (Tropical Rainfall Measuring Mission)

TRMM was launched in 1997 (Kummerow et al. 1998, 2000) and ended its mission in 2015. The most widely used satellite precipitation data are the TMPA (TRMM Multi-satellite Precipitation Analysis) 3B42 v.7 precipitation dataset that are obtained combining TRMM precipitation radar (PR), passive microwave (PMW), and infrared (IR) estimates at a three

hourly interval and 0.25° spatial resolution in the 50°S-50°N area. (Bolvin and Huffman, 2015). The TMPA rainfall is widely applied in different branches of the earth sciences, especially in data-sparse regions (e.g Awadallah and Awadallah, 2013, Khan et al. 2011, Asante et al. 2008, Bindlish et al., 2003). Details on the data product can be found in Huffman et al., 2007, 2010.

2.2 MODIS (Moderate Resolution Imaging Spectroradiometer)

Normalized Difference Vegetation Index (NDVI) and evapotranspiration (ET) are available from the Moderate Resolution Imaging Spectroradiometer (MODIS). The MODIS sensor is onboard both the Terra and Aqua satellite platforms, which were launched on December 1999 and on May 2002, respectively, in a sun-synchronous polar orbit, with estimated equatorial crossing times of 10:30am (Terra) and at 1:30pm (Aqua). MODIS provides 44 global data products for land, ocean, and atmospheric variables. Details of the MODIS land data are available at the MODIS website (http://modis.gsfc.nasa.gov), and the products used in this study, NDVI and Evapotranspiration are available as MOD13C2 and MOD16 respectively from the Land Processes Distributed Active Archive Center website (http://lpdaac.usgs.gov) and the Numerical Terradynamic Simulation Group at the University of Montana (http://www.ntsg.umt.edu/project/mod16). The algorithms to derive these products are well established and extensively evaluated: NDVI (Rouse Jr. et al 1973, Tucker, 1979; Myneni et al., 1995) and evapotranspiration (Mu et al. 2007, 2011). The monthly composite global products are available from LPDAAC on a 5.6km global Climate Modeling Grid (CMG), although local-tiled versions are available from some products at higher spatial resolutions, for example NDVI at a 1km resolution, not used in this study. The MODIS ET product is based on the Penman-Monteith method (Mu et al. 2011). There have been numerous validations of MODIS Evapotranspiration estimates in many regions of the world. Kim et al. 2012 have carried out validation of the MODIS ET

products over different land cover and climate in Asia and found that it resembled closely to the ET measured from flux towers in Australia (Cleugh et al. 2007) and Pan-Arctic (Mu et al. 2009).

2.3 GRACE (Gravity Recovery and Climate Experiment)

The U.S./German Gravity Recovery and Climate Experiment (GRACE) satellite mission was launched in 2002 to provide estimates of changes in total terrestrial water storage (represented as the sum of groundwater, soil moisture, snow, and surface waters) at large spatial scales and on a monthly basis (Tapley et al., 2004). While this mission provided monthly TWS estimates through Jan 2017, the GRACE Follow-On mission is expected to support future research using this data variable. Members of our team have developed and applied an approach for assimilating observations of soil moisture and terrestrial water storage from satellite-based sensors including GRACE into a land surface models, which have been shown to produce estimates of variations in the components of terrestrial water storage that are both accurate and as high resolution as the model grid (Bolten et al., 2010; Bolten et al., 2012; Gupta et al., 2015). The GRACE assimilation approach has been used to provide enhanced estimates of hydrological monitoring and groundwater storage by constraining terrestrial water balance (Zaitchik et al. 2008, Forman et al. 2012, Houborg et al. 2012, Li et al. 2012, Eicker et al. 2014). By including monthly observations of the terrestrial water storage in our land surface modeling scheme, it is possible to more accurately monitor regional hydrological states and fluxes, and thus calculate with more certainty the anomalies of these states and fluxes for enhanced monitoring of hydrological and agricultural drought. GRACE has been instrumental in numerous water balance studies pointing to declines in the water storages specifically the decline in groundwater in many parts of the world (Rodell et al. 2004, 2007, 2009; Tiwari et al. 2009; Landerer and Swenson, 2012), but studies cannot be conducted at smaller scales due to the coarse resolution of the sensor (Alley and Konikow, 2015; Lakshmi, 2016).

2.4 GLDAS (Global Land Data Assimilation System)

178 The Global Land Data Assimilation System (GLDAS) provides high resolution maps of land
179 surface states and fluxes by forcing modern, offline land surface models (e.g., NOAH: Ek. et al.
180 2003) with high quality observational data (Mitchell et al., 2004). The forcing data (Cosgrove at
181 al., 2003; Luo et al. 2003) and outputs have been extensively validated (Lohmann et al., 2004;
182 Robock et al., 2003; Schaake et al., 2004). The outputs are available at a 1/8^{o} spatial resolution and
183 hourly time step for the North American (NLDAS) version not used in this study, and at a 1/4^{o}
184 spatial resolution and 3-hourly time step for GLDAS. The data for both N/G-LDAS are available
185 at monthly timescales which will be used here. The LDAS data sets are described in detail at
186 http://ldas.gsfc.nasa.gov/ and http://disc.sci.gsfc.nasa.gov/hydrology/. We use the root zone soil
187 moisture (0-2m) and runoff from the improved GLDAS version 2 product in this study.
188
189 *2.5 Major River basins of the world*
190 The major river basins of the world are shown in Figure 1. These basins were extracted from
191 the Food and Agriculture Organization of the United Nations Major Hydrological Basins shapefile,
192 derived from the USGS HydroSHEDS and HYDRO1k elevation products (FAO-UN, 2015).
193 Previous studies about the basins as well as climate, area, latitudinal location, annual average
194 precipitation and air temperature are listed in Table 2. This table enables us to understand on a
195 comparative basis, the physical and climatological differences between the large river basins
196 distributed between all continents. These basins were chosen for this study because of they
197 represent a diverse climatology such as tropical, humid, semi-arid, arid and marine and the fact that
198 the hydrology and availability of water in these basins is an issue for millions of its inhabitants for
199 agriculture, hydropower, transportation and domestic and industrial uses. The annual average
200 precipitation ranges from a low of 160mm in the Colorado River basin to a high of 2,110mm for
201 the Ganga-Brahmaputra River basin. The average annual air temperature varies between 284K in
202 the Danube River basin to 300K in the Nile River basin. There is also a large variability in the size
203 - the smallest basin – California basin (California is the integrated basin for Sacramento, San

Joaquin River, Tulare Lake, , San Francisco Bay, part of North and South Coast, North and South Lahontan and the Colorado River) (400,000 km^2) to the largest – the Amazon River basin (5,000,000 km^2). Such diversity in location and climate result in a different distribution of precipitation into evapotranspiration, infiltration/recharge, runoff and soil moisture. The previous studies for each basin focus on the variability of these hydrological components and some of these have already been referenced in the introduction section.

3.0 Application of the Remotely Sensed and Modeled Data to Estimate Water Storage

3.1 Validation of the Precipitation, Evapotranspiration, and Runoff Data

Before and after the launch of earth observing satellites, studies are conducted to ensure the quality of the observations, often consisting of field studies and comparison with in-situ measurements, as well as comparisons with other remotely sensed products and modeled outputs. The TRMM retrieved precipitation, MODIS derived evapotranspiration and the GLDAS modeled runoff have been independently validated (as shown in Table 3) and can be used as proxies for direct, ground measurements. To demonstrate their local efficacy, we compare the satellite-based data sets with point-based in-situ measurements and assess the correlations by latitude, showing spatial variations of ground data in Figure 2. In the analysis, three data sets (i.e. precipitation, runoff and ET) were used: the Global Historical Climatology Network (GCHN) was compared with TRMM precipitation, runoff data from the Global Runoff Data Centre (GRDC) was compared with GLDAS NOAH runoff, and FluxNet station data were converted into ET using the Penman-Monteith equation to compare with MODIS ET (Lawrimore et al 2011; GRDC 2017; FluxNet 2015; Zotarelli et al 2010). Each of the data sources available had data that were outside of the temporal study domain, and therefore some stations could not be included in the comparison. Of the 72,882 total precipitation stations available from GCHN, only 11,286 stations had at least ten years of data within 1998-2015 to match the TRMM data; of the 9,236 discharge stations available from GRDC, only 3,540 stations could be used; finally, there are approximately 166 FluxNet

stations available globally, but only 36 stations could be compared with the MODIS Evapotranspiration. Figure 2 demonstrates how well the satellite measurements compare with traditional ground measurements. TRMM provides precipitation data from 50ºN-50ºS. The areas outside this range are masked out. The satellite direct and indirect observations closely align with measurements from ground stations, the modeled runoff data suffers drawbacks due to large grid sizes and largely ignore water management practices. In spite of these drawbacks, modeled runoff data are used in this analysis to leverage their global coverage and temporal continuity.

3.2 Hydrological balance

We carried out a basin averaged water balance and compared it to the GRACE water equivalent thickness anomaly

$$\overline{P} - \overline{ET} - \overline{R} = \overline{\Delta S} \qquad (1)$$

Where precipitation P, evapotranspiration ET, runoff R, and change in surface and subsurface water storage ΔS are monthly and basin averaged values for each of the basins. Quantities enhanced or reduced due to water withdrawals (due to irrigation, domestic and industrial uses) are not explicitly included on either side of this equation, as there was not a globally consistent method of estimation for them. All the variables on the left-hand side of equation (1) can be estimated using either satellite (P, ET) or model (R) data sets. The total change in water storage/total water on the right-hand side of the equation (ΔS) can be estimated by GRACE observations. The difference between P-ET-R and ΔS would represent the amount of withdrawal of groundwater in the basin. There does not exist any database for estimation of W and the value of W differs between basins – in regions of sufficient water supply there is not much water withdrawal. As W is seldom measured and is much smaller compared to ΔS, we have not included it in equation 1. We provide a discussion of this in section 4.

Figure 3a, b represents spatial average monthly P-ET-R and the GRACE water equivalent thickness anomalies, as water storage anomalies (for GRACE the anomalies were calculated with the 2004-2010 baseline, for all other variable, the anomalies were calculated for the length of record 2001-2015), for all the river basins studied in this paper in time series and scatter plots. There are two common features in all these basin trends. Firstly, there is a marked seasonal variability of both P-ET-R and the total water for most of the river basins but there are a few exceptions. For example, the Congo, the Colorado and the Murray-Darling River basins do not show the seasonal signal for P-ET-R and GRACE water equivalent thickness as compared to the Amazon or the Ganga-Brahmaputra River basin. The time period of the lag varies between one to 3 months and is dependent on the size and climate of the basin and the transport and storage of water. The magnitude of the P-ET-R is strongly dependent on the climate and ecosystem and this magnitude is much larger for the Amazon and the Mekong River basins as compared to the Colorado, the Murray-Darling and the Danube River basins. Direct comparison of the magnitudes of P-ET-R and the GRACE water equivalent thickness anomaly (as total water) is not possible as the former is a direct measure and the latter is an anomaly. However, the temporal variability (changes between month to month) between P-ET-R and the GRACE water equivalent thickness anomaly is justified as they both reflect the increase or decrease in the storage. A positive P-ET-R corresponds to a positive value of the GRACE water equivalent thickness anomaly and vice-versa. Examination of the correlation statistics in Table 4 (all values are significant at p value of 0.05) shows that the high correlation between P-ET-R and total water is seen for the tropical watersheds of the Amazon, the Ganga-Brahmaputra, and the Mekong River basins of 0.8 or higher and a lag of 1 month. The next group is the urban California and the Danube River basins at 0.7 or higher with 0 lags. The other basins have lower R^2 and the time lag corresponding to the maximum R^2 at 3 months in the case of the Colorado.

3.3 Co-variability of hydrological cycle components

Five variables are derived from three different sources: precipitation from TRMM, total water from GRACE, evapotranspiration, and NDVI from MODIS and runoff and soil moisture from GLDAS. The spatial resolution for precipitation (TRMM), runoff (GLDAS) and soil moisture (0-2m, GLDAS) is 0.25º, ET, and NDVI (MODIS) is 0.05º and that of total water (GRACE) is 1º. Figures 4 and 5 represent the monthly time series of the water balance components for the Mekong and the Murray Darling River Basins respectively. These include, monthly anomaly time series for (a) precipitation (b) runoff (c) soil moisture (d) ET and (e) total water as GRACE water equivalent thickness anomaly. The anomalies for precipitation, ET, runoff and soil moisture are calculated using January 2001 to December 2014 period as a baseline. The figures highlight the seasonal and annual variability of the hydrological cycle between January 2001 and December 2014 (the total water time series starts in April 2002 corresponding to the GRACE launch). Also indicated in these figures are the high negative and positive anomalies that correspond to dry (drought) and wet (flood) conditions in the basin. Examination of these time series shows that the co-variability of these four components of the hydrological cycle follows the water balance. We chose for the Mekong River Basin (Figure 4) and the Murray Darling River Basin (Figure 5) dry and wet months based on low and high GRACE water equivalent thickness anomaly. If we examine Figure 4(a)-(e) we observe that one of the periods of lowest precipitation in the Mekong River Basin corresponds to January 2005 with a precipitation anomaly of -0.5mm corresponding to a 0mm and -7.5mm for the runoff anomaly and ET anomaly respectively in March 2005 (lags rainfall by 2 months) and -3.5mm for soil moisture and -100mm for the total water in May 2005. The other extreme corresponds to the extremely wet month of September 2011 with a positive anomaly for rainfall of +100mm and a corresponding positive anomaly of runoff of +5mm, soil moisture of 5mm and (lagged by one month – October 2011), total water anomaly of +100mm (November 2011, lag of two months) and the ET shows generally positive anomalies a few months later starting in December 2011 for a period of over 12 months. The correspondence of the rainfall to runoff, soil moisture and total water is well displayed in this figure. The same findings hold for the Murray

Darling River Basin – the dry and wet periods are related between all of the variables displayed in Figure 5. The dry period of low rainfall (-75mm) and runoff (0mm) in August 2009 corresponds to low soil moisture (-3mm), ET (-10mm) and low total water (-50mm) in November 2009; the wet period with above normal rainfall (+70mm) corresponds to December 2010 and positive runoff (+2mm) and soil moisture (+15mm) in February 2011 and high total water (+100mm) in March 2011. The ET shows a high positive anomaly of +25mm for December 2010 and remains positive for several months. In Figure 4a we observe that the precipitation has a negative anomaly throughout the Mekong River Basin for January 2005 and as a result both the soil moisture and runoff two months later (March 2005) show negative anomalies and the total water in May 2005 shows negative anomalies ranging from -100mm to -500mm throughout the catchment. The same is true for the spatial distribution of the positive anomalies for precipitation extends to soil moisture, runoff, ET and total water that has a positive anomaly ranging from 200mm to 500mm in the southern part of the Mekong River Basin. Similar spatial patterns are seen for the Murray Darling River Basin.

On examination of the total water for the Murray Darling Basin (Figure 5e), it is seen that it shifts from mostly negative to positive values at the beginning of 2010. This is expected, as the rainfall (Figure 5a) exhibits high values positive anomalies in six months of 2010 (+60mm) as well as in January and February 2012. These high positive anomalies in rainfall during 2010 (coupled with lower values of ET) keep the water balance positive in the basin.

One of the most important observations that can be seen from Figures 4(a)-(e) and 5(a)-(e) in the spatial maps of the catchment for the hydrological cycle variables is the sharp contrast between the dry and the wet periods. The spatial pattern of the variables for the wet month are dominated by positive rainfall, soil moisture, runoff, ET and total water anomalies and vice-versa for the dry months.

3.4 Spatial variability

Examination of the spatial variability of the hydrological cycle variables in two river basins – the Amazon and the Colorado (Figure 6) yields interesting and contrasting results.

Figure 6 displays the monthly spatial standard deviation of precipitation (TRMM), runoff (GLDAS), ET (MODIS), soil moisture (GLDAS) and total water anomaly (GRACE) (all in mm). The differences between the Amazon and the Colorado with respect to spatial variability are very apparent. To begin with, the spatial variability of the precipitation in the Colorado River basin varies between 0 and 30mm whereas for the Amazon River basin the range is between 60 and 180mm. This spatial variability in precipitation translates to a larger spatial variability in runoff for the Amazon River basin (2-30mm) as compared to the Colorado River basin (0-10mm). The standard deviation of the precipitation for the Amazon River basin generally shows a minimum in months of August and September (around 60mm) a maximum in the month of May (between 150-180mm). The spatial variability of runoff for the Amazon River basin is lowest in July and August (standard deviation of around 5mm) and highest in January-March (20-30mm). The spatial variability of evapotranspiration shows a distinctive seasonal signature for both the Amazon and the Colorado River basins. For the Amazon, there is a variation between a minimum in the month of February of 15mm and a maximum in the months of August and September of around 35mm. In the case of the Colorado River basin the minimum spatial variability is in the winter months (December to February) of 5mm and a maximum during the summer months of June and July of 20mm. It can be noticed that in the case of the Amazon River basin the maximum standard deviation for runoff corresponds to the minimum standard deviation for ET. The spatial variability for soil moisture for both the Amazon and the Colorado River basins does not show any seasonal variability with the spatial standard deviation for the Amazon River basin being higher (between 13 and 22m) as compared to the Colorado River basin (between 6 and 12mm). The variability of total water for the Amazon River basin shows a very large range (between 100mm and 400mm) as compared to the Colorado River basin (between 0 and 80mm).

358 Examination of the spatial variability of precipitation, NDVI and ET in January 2005 and
359 June 2005 for the Colorado River Basin and January 2005 and August 2005 for the Amazon River
360 Basin shows remarkable differences between the two basins (Figure 7 and 8 respectively). Whereas
361 most of the Colorado River basin has little or no vegetation in January 2005 (NDVI around 0.15
362 and only a small region in the southern part with any vegetation), the Amazon River basin shows
363 larger extent of greenness (large region NDVI around 0.7). There is a large spatial variability in ET
364 for the Amazon River basin between 0 and 150mm and much lower range for the Colorado River
365 basin (between 10 to 40mm). The difference in ET in August 2005 for the Amazon River basin
366 between the south and the north is evident from the very low ET in the southern part of the basin
367 (0-20mm) contrasting with the high ET (120-150mm) in the northern part of the basin. In the
368 Amazon River basin, this is strongly related to the higher amount of vegetation and the rainfall in
369 the north (NDVI 0.7 to 0.9 in the north and 0.5 to 0.8 in the south; rainfall of 150-250mm in the
370 north and 0-75mm in the southern part of the basin). This is in stark contrast to the spatial pattern
371 of ET for the Amazon River basin which is much more uniform across the region as also reflected
372 in rainfall and vegetation. The large difference in ET in June 2005 in the Colorado River basin
373 between the northeast and the south is also seen (Figure 7) and it varies between 0 and 80mm across
374 the basin and is strongly related to the variation of NDVI (0.15-0.75) with higher NDVI in the
375 northeast (0.70) and much lower in the south (0.15) and rainfall is much higher in the northeast
376 (60mm) and much lower in the south (less than 10mm).
377
378 *3.5 Temporal variability: Anomaly index analysis*
379 The data analyzed in this paper spans over 15 years and 11 river basins of the world. Whereas
380 each of these river basins has been studied in considerable detail in many past studies (Table 2), a
381 comprehensive comparison has never been undertaken. In considering locations with differing
382 annual rainfall, temperature and land cover direct comparisons will not yield quantitative results
383 due to obvious differences between basins. For example, there is always greater rainfall and runoff

384 in the Amazon River basin as compared to the Murray Darling River basin. In order to overcome
385 this problem, we have constructed the anomaly index defined as the monthly anomaly divided by
386 the monthly climatology. As the anomaly index normalizes the monthly anomaly by dividing by
387 the monthly climatology, the regions with anomaly index would measure the variability of the
388 monthly anomaly as a fraction of the monthly climatology value. For example, when we compare
389 the Amazon with high monthly rainfall to the Murray Darling basin with much lower rainfall using
390 the precipitation anomaly index, we are only comparing the fraction of variability. The minimum
391 and maximum monthly anomaly index values are presented in Table 5.

392 Figure 9 shows the comparison of precipitation using the anomaly index for the Amazon River
393 basin and the Murray-Darling basin. Whereas the index values in the Amazon River basin range
394 from -0.4 to 0.61, the index values for the Murray-Darling basin varies between -0.95 and 1.73
395 (Table 5). The temporal variability of this index for the Amazon is 0.11 and for the Murray-Darling
396 is 0.52. Both these statistics show that the variability of the monthly rainfall as a ratio of the monthly
397 rainfall climatology is much higher in the Murray-Darling basin and is subject to greater extremes
398 in precipitation. These are periods when the rainfall is below normal (negative precipitation
399 anomaly index), which is seen between 2001 and 2009 and this period corresponds to a severe
400 drought in the region. We observe a period of high monthly precipitation (compared to the
401 climatology) for 2010 and 2012 and November 2010 corresponds to a large-scale flood in this
402 region. In the case of the Amazon River basin there is very little deviation of the precipitation
403 anomaly index from zero (zero indicates no departure from the monthly climatology) and hence
404 the river basin is not subject to extremes. A few other river basins with large negative precipitation
405 anomaly index (and hence subject to droughts) are the California, the Colorado, the Danube, and
406 the Ganga-Brahmaputra River Basins. The monthly anomaly indices between different variables
407 capture the connection between the land surface variables. The variability in vegetation index is
408 connected to the variability of the evapotranspiration. The Amazon River basin shows a low range
409 of NDVI (-0.04 to 0.08) and a corresponding low range for ET (-0.17 to -0.29). However, the

Murray-Darling basin shows a much larger range for NDVI variation (-0.23 to 0.38) and a corresponding higher range for ET (-0.63 to 1.7). This is shown in Figure 9 and Table 5. Table 5 shows the minimum and maximum monthly values for the anomaly index. The temporal standard deviation for monthly NDVI anomaly index is 0.02and 0.12 and monthly ET anomaly index is 0.04 and 0.29 for the Amazon River basin and the Murray-Darling basin respectively. Larger variability in precipitation translates to greater variability in NDVI and ET for the Murray-Darling basin as compared to the Amazon River basin.

4.0 Conclusions and Discussion

We have examined the water balance components for eleven global river basins using publicly available monthly satellite data and model output products for a period of 15 years between 2001 and 2015. The water balance components of the hydrological cycle include precipitation, ET, soil moisture, runoff, and total water. The river basins are located in contrasting climate, topography and ecosystems across the globe in all continents (with the exception of Antarctica). In comparing the output of P-ET-R to the changes associated with the total water (from GRACE) we observe a distinct seasonal cycle with a maximum lag of a few months between the two quantities (P-ET-R and ΔS). The correlation between P-ET-R and total water change shows a large variability among basins with the highest being the Amazon River basin at R^2 of 0.9 and lowest at R^2 of ~0.35 for the Colorado River and the Murray-Darling River basins. The differences between the basins may stem from the human engineering of the water systems in the basin; the Amazon River basin has been subject to much less human intervention compared to the Colorado and the Murray-Darling River basins. Another factor in this difference is the storage and melting of snow in some basins. We compared a month of wet with a dry month for the Mekong River and the Murray Darling River basin. On comparison of precipitation, runoff, soil moisture, ET and total water we find a consistency in the hydrological cycle with respect to the water balance; i.e. we find for wet/flood periods – a large positive anomaly of precipitation from TRMM corresponding to

positive anomalies of ET from MODIS, runoff and soil moisture from GLDAS and total water from GRACE and vice-versa for negative anomaly or dry/drought conditions. Finally, we compute the anomaly index and compare these variables across river basins. The precipitation anomaly index for the Amazon River basin has a much lower variability compared to the Murray Darling River basin. The anomaly indices of the other hydrological variables are also compared with each other and across basins and this leads to very consistent relationship.

Equation 1 in section 3.2 has an implicit withdrawal term which presents us with a problem. Whereas in principle, Equations 1 and 2 should be balanced if all the individual variables are perfect maintaining a water balance, this is not the case as seen in the results in Figures 3(a)-(k). We therefore conclude that the problem in this balance equation is the fact that the individual variables are not perfect and compounding the fact is that the withdrawal terms on both sides of the equation are seldom known. The dynamics of withdrawal is very complicated. Withdrawal due to irrigation can either (a) leave the watershed as evapotranspiration or runoff and this is accounted for in the equation, (b) infiltrate into the soil and recharge the groundwater, or (c) leave the system through domestic water withdrawal and subsequent transport elsewhere. Each of these has to be treated separately and one treatment would not address all physical mechanisms. Therefore, we have removed the withdrawal term in Equation 1 as we have realized that the accuracies of the individual terms in equation (1) probably account for withdrawal. However, a much more involved analysis needs to be undertaken and this would need to be done at (a) the whole river basin scale and (b) sub-basins to determine the actual dynamics. We hope that this will be the subject of further studies.

In this paper, we utilize monthly data from satellites and models over a 15-year period for analysis. This study is unique as it is (a) multi-year period using a combination of publicly available satellite data and model output (b) comparison of river basins across the globe located in a range of climate, topography and ecosystems. Though the data come from different sources, they display the required relationship with each other to complete a hydrological balance. In addition, the

462 hydrological variables display very interesting spatial and temporal patterns that are consistent with
463 hydrological extremes of floods and droughts. In the future, such studies will be very important to
464 determine availability of water resources under the growing pressures of an ever-increasing
465 population. Studies like this present work when carried out at higher spatial resolution will aid and
466 assist local agencies for improved land use and water use management. Understanding variability
467 of the different components of the water budgets for the past 20 years will help in the planning for
468 the net 20 years.

469 In many countries of the world where these major river basins are located, the rivers are
470 the economic engine of the communities – agriculture, industry, transportation, power production
471 and water supply and predicting the water resources, including their inter-annual and inter-seasonal
472 variability, is essential to assessing water availability and is useful for planning in case of extreme
473 hydrological events of floods and droughts. Observations of water in many developing countries
474 of the world are constrained by lack of adequate gauge stations. Many agencies that collect the
475 streamflow or precipitation data internationally are not likely to share this data with others due to
476 national security policies of their respective governments, which makes comprehensive analysis
477 using these data sets very difficult. Satellite remote sensing and use of global land model data sets
478 can help in this regard. This study showed several examples of how satellite remote sensing can be
479 used over large areas and long-time periods to identify spatial and temporal variation, as well as
480 how to estimate total water fluctuations using a simple water balance model, and how to compare
481 hydrologic phenomena across hydrologic regions. However, we stress two important points in this
482 regard. One - there is no substitute for in-situ observations of precipitation, evapotranspiration and
483 stream flow especially for small catchments to perform water balance as well as test theories and
484 equations that can be used for larger spatial scales. Two – validation studies are usually carried out
485 at smaller scales (catchments on the order of a few 1000 km^2) and for the large catchments such as
486 those in this present study, there are really no distributed validation studies. For these reasons, we
487 rely on the use of standard validated data sets. Future studies seek to develop models to complete

488 these analyses at even finer spatial resolution which will serve the international community at more
489 local scales.
490
491

Acknowledgements

The authors wish to acknowledge the support of Dr. Bradley Doorn, Program Manager, Water Resources, Applied Sciences Program (award number 80NSSC18K0433) and Dr. Jared Entin, Program Manager, Terrestrial Hydrology (Award number NNX12AP75G) at NASA Headquarters for funding this research.

References

Adler R.F., Huffman G.J., Bolvin D.T., Curtis S., and Nelkin E.J. 2000. Tropical Rainfall Distributions Determined Using TRMM Combined with Other Satellite and Rain Gauge Information. *Journal of Applied Meteorology and Climatology*.

Aerts, J., H Renssen, P Ward, H de Moel, E Odada, L Bouwer and H Gossee, 2006, Sensitivity of global river discharges under Holocene and future climate conditions, *Geophysical Research Letters*, 33(19), L19401, DOI 10.1029/2006GL027493

Alcamo, J., M. Florke and M. Marker, Future long-term changes in groundwater resources driven by socio-economic and climatic changes, *Hydrological Sciences Journal*, 52(2), pp247-275, 2007

Alley, W. and L Konikow, Bringing GRACE down to earth, Technical commentary, *Groundwater*, DOI 10.1111/gwat.12379, 2015

Arnell, N., 1999, Climate change and global water resources, *Global Environmental Change – Human and Policy Dimensions*, Vol. 9, Supplement S, pp. S31-S49

Amitai E., Wolff D., Marks D., Silberstein E. 2002. Radar rainfall estimation: lessons learned from the NASA/TRMM validation program. *Proceedings of ERAD 2002*.

Asante, K. O., G. A. Arlan, S. Pervez, and J. Rowland, 2008, A linear geospatial stream- flow modeling system for data sparse environments, *International Journal of River Basin Management*, 6 (3), pp. 233-241

Awadallah, A. G., and N. A. Awadallah, 2013, A novel approach for the joint use of rainfall monthly and daily ground station data with TRMM data to generate idf estimates in a poorly gauged arid region, *Open Journal of Modern Hydrology*, 3 (01), pp. 1-7

Barnett, T., R Malone, W Pennell, D Stammer, B Semtner, W Washington, 2004, The effect of climate change on water resources in the west: Introduction and Overview, *Climatic Change*, 62, 1-3, pp. 1-11

Bindlish, R., T. J. Jackson, E. Wood, H. Gao, P. Starks, D. Bosch, and V. Lakshmi, 2003, Soil moisture estimates from TRMM microwave imager observations over the southern united states, *Remote Sensing of Environment*, 85 (4), 507–515.

Bolten, J., W. Crow, X. Zhan, C. Reynolds, T. Jackson, 2010, Evaluating the Utility of Remotely-Sensed Soil Moisture Retrievals for Operational Agricultural Drought Monitoring, *IEEE Journal of Selected Topics in Applied Earth Observations and Remote Sensing*, Vol. 3 No. 1, pp. 57-66

Bolten, J., and W. Crow. 2012. "Improved prediction of quasi-global vegetation conditions using remotely-sensed surface soil moisture." *Geophysical Research Letters*, 39 (19): L19406 [10.1029/2012GL053470]

Bolvin, D., and G. Huffman, 2015, Transition of 3b42/3b43research product from monthly climatological calibration/adjustment, Technical Notes, NASA, Washington, DC 20546.

Christensen, N., A Wood, A Voisin, D Lettenmaier and R Palmer, 2004, The effect of climate change on the hydrology and water resources of the Colorado River Basin, *Climate Change*, 62, 1-3, pp. 337-363

Christensen, N. and D Lettenmaier, 2007, A multimodel ensemble approach to assessment of climate change impacts on hydrology and water resources of the Colorado River Basin, *Hydrology and Earth System Sciences*, 11(4), pp. 1417-1434

Cleugh, H., R Leuning, Q Mu and S Running, 2007, Regional evaporation estimates from flux tower and MODIS satellite data, *Remote Sensing of Environment*, Vol. 106, No. 3, pp. 285-204

Conway D, 1997, A water balance model of the Upper Blue Nile in Ethiopia, *Hydrological Sciences Journal*, 42(2), pp. 265-286

Cosgrove, B., and coauthors, 2003, Real-time and retrospective forcing in the North American Land Data Assimilation System (NLDAS) Project, *Journal of Geophysical Research*, 108(D22), 8842, doi:10.1029/2002JD003118.

Dai, A., T Qian, K Trenberth and J Millman, 2009, Changes in continental freshwater discharge 1948-2004, *Journal of Climate*, 22(10), pp. 2273-2792

Dettinger, M., D Cayan, M Meyer and A Jeton, 2004, Simulated hydrologic responses to climate variations and change in Merced, Carson and American River Basins, Sierra Nevada, California 1900-2099, *Climate Change*, 62, No. 1-3, pp. 283-317

Donohue, R., M Roderick, T McVicar, 2011, Assessing the differences in sensitivities of runoff to changes in climatic conditions across a large basin, *Journal of Hydrology*, 406 (3-4), pp. 234-244

Eicker, A., M Schumacher, J Kusche et al., 2014, Calibration/Data Assimilation approach for integration GRACE data into WATERGap Global Hydrology Model (WGHM) Using Ensemble Kalman Filter: First Results, *Surveys of Geophysics*, 35: 1285, doi:10.1007/s10712-014-9309-8

Ek, M. B., K. E. Mitchell, Y. Lin, E. Rogers, P. Grunmann, V. Koren, G. Gayno, and J. D. Tarpley, 2003, Implementation of Noah land surface model advances in the National Centers for Environmental Prediction operational mesoscale Eta model, *Journal of Geophysical Research*, 108(D22), 8851, doi:10.1029/2002JD003296.

Elshamy, M., I Seierstad and Sorteberg, 2009, Impacts of climate change on Blue Nile flows using bias-corrected GCM scenarios, *Hydrology and Earth System Sciences*, 13(5), pp. 551-565

Food and Agriculture Organization of the United Nations. FAO GEONETWORK. World map of the major hydrological basins (Derived from HydroSHEDS) (GeoLayer). (Latest update: 04 Jun 2015) *url*: http://data.fao.org/ref/7707086d-af3c-41cc-8aa5-323d8609b2d1.html?version=1.0

Forman, B., R Reichle, M Rodell, 2012, Assimilation of terrestrial water storage from GRACE in a snow dominated basin, *Water Resources Research*, 48(1), doi:10.1029/2011WR011239

Frappart, F., and others, 2006, Water volume change in the lower Mekong from satellite altimetry and imagery data, *Geophysical Journal International*, 167(2), pp. 570-584

Fluxnet 2015, http://fluxnet.fluxdata.org/data/fluxnet2015-dataset/

Gebremichael M., and Krajewski W.F. 2004 Assessment of the Statistical Characterization of Small-Scale Rainfall Variability from Radar: Analysis of TRMM Ground Validation Datasets. *Journal of Applied Meteorology and Climatology*.

Gemitzi A., Ajami H., Richnow H.H. 2017. Developing empirical monthly groundwater recharge equations based on modeling and remote sensing data – Modeling future groundwater recharge to predict potential climate change impacts. *Journal of Hydrology*

GRDC, Global Runoff Data Center, http://www.bafg.de/GRDC/EN/Home/homepage_node.html

Guo, S., J Wang, L Xiong, A Ying and D Li, 2002, A macro-scale and semi-distributed monthly water balance model to predict climate change impacts in China, *Journal of Hydrology*, 268(1-4), pp. 1-15

Gupta M., J Bolten and V Lakshmi, Use of Satellite-Based Water Cycle Observations for improved soil hydraulic properties**,** Under review, *Vadose Zone Journal*, 2015

Herrera-Pantoja, M. and K. Hiscock, The effects of climate change on potential groundwater recharge in Great Britain, *Hydrological Processes*, 22, pp 73-86, 2008

Houborg. R., M Rodell, B Li, R Reichle and B Zaitchik, 2012, Drought indicators based in model-assimilated Gracity Recovery and Climate Experiment (GRACE) terrestrial water storage observations, *Water Resources Research*, 48(7), doi:10.1029/2011WR011291

Huffman, G. J., D. T. Bolvin, E. J. Nelkin, D. B. Wolff, R. F. Adler, G. Gu, Y. Hong, K. P. Bowman, and E. F. Stocker, 2007, The TRMM multisatellite precipitation analysis (TMPA): Quasi-global, multiyear, combined-sensor precipitation estimates at fine scales, *Journal of Hydrometeorology*, 8 (1), pp. 38–55

Huffman, G.J., R.F. Adler, D.T. Bolvin, E.J. Nelkin, 2010, The TRMM Multi-satellite Precipitation Analysis (TMPA), Chapter 1 in Satellite Rainfall Applications for Surface Hydrology, F. Hossain and M. Gebremichael, Eds. Springer Verlag, ISBN: 978-90-481-2914-0, pp. 3-22

Jha, M., J Arnold, P Gassman, F Giorgi and R Gu, 2006, Climate change sensitivity assessment on Upper Mississippi River Basin streamflow using SWAT, *Journal of American Water Resources Association*, 42(4), pp. 997-1105

Justice et al 1998, The Moderate Resolution Imaging Spectroradiometer (MODIS): Land Remote Sensing for Global Change Research, *IEEE Transactions on Geoscience and Remote Sensing*, 36(4), pp. 1228-1249

Justice et al. 2002, An overview of MODIS land data processing and product status, *Remote Sensing of Environment*, 83, pp. 3-15

Karl, T. R., Kukla, G., Gavin, J, 1984, Decreasing diurnal temperature range in the United States and Canada from 1941 through 1980, *Journal of climate and applied meteorology*, 23(11), pp. 1489-1504.

Khan, S., P. Adhikari, Y. Hong, H. Vergara, R. F Adler, F. Policelli, D. Irwin, T. Korme, and L. Okello, 2011, Hydroclimatology of lake victoria region using hydrologic model and satellite remote sensing data,

Hydrology and Earth System Sciences, 15 (1), 107

Kim H.W., Hwang K., Mu Q., Lee S.O., Choi M. 2012. Validation of MODIS 16 global terrestrial evapotranspiration products in various climates and land cover types in Asia. *KSCE Journal of Engineering*.

Kingston, D., J Thompson and G Kite, 2011, Uncertainty in climate change projections of discharge for Mekong River Basin, *Hydrology and Earth System Sciences*, 15(5), pp. 1459-1471

Kite, G., 2001, Modeling the Mekong: hydrological simulation for climate impact studies, *Journal of Hydrology*, 253(1-4), pp. 1-13

Klein, B., I Lingemann, E Nilson, P Krahe, T Maurer and H Moser, 2012, Key concepts for analysis of climate change impacts for river basin management in the River Danube, *River Systems*, 20(1-2), pp. 7-21

Kummerow C., Barnes W., Kozu T., Shiue J., Simpson J., 1998, The Tropical Rainfall Measuring Mission (TRMM) Sensor Package. *Journal of Atmospheric and Oceanic Technology*.

Kummerow, C., J Simpson, O Thiele and others, 2000, The status of Tropical Rainfall Measurement Mission after two years in orbit, *Journal of Applied Meteorology*, 39(12), pp. 1965-1982

Kundzewicz, Z.W., L.J. Mata, N.W. Arnell, P. Döll, P. Kabat, B. Jiménez, K.A. Miller, T. Oki, Z. Sen and I.A. Shiklomanov, 2007: Freshwater resources and their management. *Climate Change 2007: Impacts, Adaptation and Vulnerability. Contribution of Working Group II to the Fourth Assessment Report of the Intergovernmental Panel on Climate Change*, M.L. Parry, O.F. Canziani, J.P. Palutikof, P.J. van der Linden and C.E. Hanson, Eds., Cambridge University Press, Cambridge, UK, pp173-210.

Lakshmi, V, Beyond GRACE: Use of satellite for groundwater investigations, Technical Note, *Groundwater*, doi: 10.1111/gwat.12444, 2016

Landerer F., and S Swenson, 2012, Accuracy of scaled GRACE terrestrial water storage estimates, *Water Resources Research*, 48, W04531, DOI 10.1029/2011WR011453

Lawrimore, J. H., M. J. Menne, B. E. Gleason, C. N. Williams, D. B. Wuertz, R. S. Vose, and J. Rennie (2011), An overview of the Global Historical Climatology Network monthly mean temperature data set, version 3, J. *Geophys. Res*., 116, D19121, doi:10.1029/2011JD016187.

Lee H., E Beighley, D Alsdorf, C Jung, C Shum, J Duan, J Guo, D Yamazaki and K Andreadis, 2011, Characterization of the terrestrial water dynamics in the Congo Basin using GRACE and satellite radar altimetry, *Remote Sensing of Environment*, 115(12), pp. 3530-3538

Li, B., M Rodell, B Zaitchik, R Reichle, R Koster and T van Dam, 2012, Assimilation of GRACE terrestrial water storage into a land surface model: evaluation and potential value for drought monitoring in western and central Europe, *Journal of Hydrology*, Vol. 446, pp. 103-115

Liao L., Meneghini R. 2009 Validation of TRMM Precipitation Radar through Comparison of Its Multiyear Measurements with Ground-Based Radar. *Journal of Applied Meteorology and Climatology*.

Lohmann D., and others, 2004, Streamflow and water balance intercomparisons of four land surface models in the North American Land Data Assimilation Project, *Journal of Geophysical Research*, Vol. 109, D07S91, doi:10.1029/2003JD003517

Luo, Y., E. Berbery, K. Mitchell and A. Betts, 2007, Relationships between land surface and near surface atmospheric variables in the NCEP Morth American Regional Reanalysis, *Journal of Hydrometeorology*, Vol. 8, pp. 1184-1203.

Marengo, J., 2005, Characteristics and spatio-temporal variability of the Amazon River Basin water budget, *Climate Dynamics*, 24(1), pp. 11-22

Mitchell (and 22 others), 2004, The multi-institution North American Land Data Assimilation System (NLDAS) Utilizing multiple GCIP products and partners in a continental distributed hydrological modeling system, *Journal of Geophysical Research*, Vol. 109, D07S90, doi:10.1029/2003

Monteith, J. L., 1965, Evaporation and Environment. In: The state and movement of water in living organism. 19th Symposium of the Society of Experimental Biology, pp. 205-234

Myneni, R.B., F.G. Hall, P.J. Sellers, and A.L. Marshak, 1995, The interpretation of spectral vegetation indexes, *IEEE Transactions* on *Geoscience and Remote Sensing* 33(2), pp. 481–486.

Mu, Q., F. Heinsch, M. Zhao and S. Running, 2007, Development of a global evapotranspiration algorithm based on MODIS and global meteorology data, *Remote Sensing of Environment*, 111, pp. 519-536

Mu, Q., L Jones, J Kimball, K McDonald and S Running, 2009, Satellite assessment of land surface evapotranspiration for pan-Arctic domain, *Water Resources Research*, Vol. 45, No. 9, W09420

Mu, Q., M. Zhao and S. Running, 2011, Improvements to a MODIS global terrestrial evapotranspiration product, *Remote Sensing of Environment*, 115(8), pp. 1781-1800

Nepal, S. and A Shreshta, 2015, Impact of climate change on the hydrological regime of the Indus, Ganges and Brahmaputra river basins: A review of literature, *International Journal of Water Resources Development*, 31(2), pp. 201-218

Nicholson S. E., Some B. , McCollum J. , Nelkin E., Klotter D., Berte Y., Diallo B. M., Gaye I., Kpabeba G., Ndiaye O., Noukpozounkou J. N., Tanu M. M., Thiam A., Toure A. A., and Traoren A. K. 2003. Validation of TRMM and Other Rainfall Estimates with a High-Density Gauge Dataset for West Africa. Part I: Validation of GPCC Rainfall Product and Pre-TRMM Satellite and Blended Products. *Journal of Applied Meterology and Climatology.*

Nijssen, B., G O'Donnell, A Hamlet and D Lettenmaier, 2001, Hydrologic sensitivity of global rivers to climate change, *Climate Change*, 50(1-2), pp. 143-175

Oki, T. and S Kanae, 2006, Global hydrological cycles and world water resources, *Science*, Vol. 313, Issue 5790, pp. 1068-1072

Piao, S., and 12 others, 2010, The impacts of climate change on water resources and agriculture in China, *Nature*, Vol. 467, Issue 7311, pp. 43-51

Pittock, J. and M Finlayson, 2011, Australia's Murray-Darling Basin: freshwater ecosystem conservation options in an era of climate change, *Marine and Freshwater Research*, 62(3), pp. 232-243

Potter, N., F Chiew and A Frost, 2010, An assessment of the severity of recent reductions of rainfall-runoff in the Murray-Darling Basin, *Journal of Hydrology*, 381(1-2), pp. 52-64

Ragab, R. and C Prudhomme, 2002, Climate change and water resources management in arid and semi-arid regions: Prospective and challenges for the 21st century, *Biosystems Engineering*, 81(1), pp. 3-34

Robock (and 15 others), 2003, Evaluation of the North American Land Data Assimilation System over the Southern Great Plains during the warm season, *Journal of Geophysical Research*, Vol. 108, NO D22, 8846, doi:10.1029/2002, JD003245

Rodell, M., P.R. Houser, U. Jambor, J. Gottschalck, K. Mitchell, C.-J. Meng, K. Arsenault, B. Cosgrove, J. Radakovich, M. Bosilovich, J.K. Entin, J.P. Walker, D. Lohmann, and D. Toll. 2004. The Global Land Data Assimilation System. *Journal of the American Meteorological Society*.

Rodell, M. and others, 2007, Estimating groundwater changes in the Mississippi River Basin (USA) using GRACE, *Hydrogeology Journal*, 15(1), pp. 159-166

Rodell, M., I Veliconga and J Famiglietti, 2009, Satellite-based estimates of groundwater depletion in India, *Nature*, 460(7258), pp. 999-U80, DOI 10.1038/nature08238

Rouse Jr., J. W., Haas, R. H., Schell, J. A., & Deering, D. W. (1973). Monitoring the Vernal Advancement and Retrogradation (Greenwave Effect) of Natural Vegetation. Greenbelt, Maryland: Goddard Space Flight Center.

Roy P., N Samal, M Roy and A Mazumdar, 2015, Integrated assessment of impact of water resources of important river basins in Eastern India under projected climate conditions, *Global Nest Journal*, 17(3), pp. 594-606

Scanlon, B., K Kesse, A Flint, L Flint, C Gaye, W Edmunds, I Simmers, 2006, Global synthesis of groundwater recharge in semi-arid and arid regions, *Hydrological Processes*, 20(15), pp. 3335-3370

Schaake (and 14 others), 2004, Intercomparison of soil moisture fields in the North American Land Data Assimilation System (NLDAS), *Journal of Geophysical Research*, Vol. 109, D01S90, doi:10.1029/2002JD003309

Singh P., M Arora and N Goel, 2006, Effect of climate change on runoff of a glacierized Himalayan basin, *Hydrological processes*, 20(9), pp. 1979-1992

Stagl, J. and F Hattermann, 2015, Impacts of climate change on the hydrological regime of the Danube River and its tributaries using an ensemble of climate scenarios, *Water*, 7(11), pp. 6139-6172

Syed, H., J Famiglietti, J Chen, M Rodell, S Seneviratne, P Viterbo and C Wilson, 2005, Total basin discharge for the Amazon and Mississippi River Basins from GRACE and land-atmosphere water balance, *Geophysical Research Letters*, 32(24), L24404, DOI 10.1029/2005GL024851

Syed, T.H., J.S. Famiglietti, M. Rodell, J.L. Chen, and C.R. Wilson. 2008. Analysis of terrestrial water storage changes from GRACE and GLDAS. *Water Resources Research*.

Szepszo, G, I Lingemann, B Klein and M Kovacs, 2014, Impact of climate change on hydrological conditions of Rhine and Upper Danube rivers based on the results of regional climate and hydrological models, *Natural Hazards*, 72(1), pp. pp. 241-262

TRMM Science Team. 2015. Rain Gauge-Disdrometer-Radar. https://gpm-gv.gsfc.nasa.gov/

Tang R., Li Z.L., Chen K.S. 2011. Validating MODIS-derived land surface evapotranspiration with in situ measurements at two AmeriFlux sites in a semiarid region. *Journal of Geophysical Research - Atmospheres*

Tapley, B., S Bettadpur, M Watkins and C Reignber, 2004, The Gravity Recovery and Climate Experiment: Mission overview and early results, *Geophysical Research Letters*, 31(9), DOI: 10.1029/2004GL019920

Taylor, R. and others, 2013, Groundwater and climate change, *Nature Climate Change*, 3(4), pp. 322-329

Tiwari, V., J Wahr and S Swenson, 2009, Dwindling groundwater resources in India from satellite gravity observations, *Geophysical Research Letters*, 36, L18401, DOI 10.1029/2009GL039401

Tshimanga, R., and D Hughes, 2012, Climate change impacts on the hydrology of the Congo Basin, *Physics and Chemistry of the Earth*, Vol. 50-52, pp. 72-83

Tucker, C.J., 1979, Red and photographic infrared linear combinations for monitoring vegetation, *Remote Sensing of the Environ*ment, 8(2), pp. 127–150

United Nations World Water Development Report, 2016, Water and Jobs, UNESCO, ISBN 978-92-3-100146-8, http://unesdoc.unesco.org/images/0024/002439/243938e.pdf

Velpuri N.M., Senay G.B., Singh R.K., Bohms S., Verdin J.P. 2013 A comprehensive evaluation of two MODIS evapotranspiration products over the conterminous United States: Using point and gridded FLUXNET and water balance ET. *Remote Sensing of Environment*.

Vorosmarty C., C Green, P Salisbury and R Lammers, 2000, Global water resources: Vulnerability from climate change and population growth, *Science*, Vol. 289, Issue 5477, pp. 284-288

Wolff D., Marks D. A., Amitai E., Silberstein D. S., Fisher B. L., Tokay A., Wang J., and Pippitt J. L. 2005. Ground Validation for the Tropical Rainfall Measuring Mission (TRMM). *Journal of Atmospheric and Oceanic Technology*.

Xu, J., D Yang, Y Yi, Z Lei, J Chen and W Yang, 2008, Spatial and temporal variation of runoff in the Yangtze River basin during the past 40 years, *Quaternary Journal*, Vol. 186, pp. 32-42

Xu, H., R Taylor and Y Xu, 2011, Quantifying uncertainty in the impacts of climate change on river discharge in the subcatchments of the Yangtze and Yellow River Basins of China, Hydrology and Earth System Sciences, 15(1), pp. 333-344

Yates, D., K Strzepek, 1998, Modeling Nile Basin under climate change, *Journal of Hydrology*, 3(2), pp. 98-108

Yates, D. and others, 2009, Climate driven water resources model of Sacramento Basin, California, *Journal of Water Resources Planning and Management*, 135(5), pp. 303-313

Zaitchik, B., Rodell, M., Reichle, R., 2008, Assimilation of GRACE Terrestrial Water Storage Data into a Land Surface Model: Results for the Mississippi River Basin, *Journal of Hydrometeorology*, Vol. 9, pp. 535-548.

Zaitchik, B.F., M. Rodell, and F. Olivera. 2010. Evaluation of the Global Land Data Assimilation System using global river discharge data and a source-to-sink routing scheme. *Water Resources Research*.

Zotarelli L., Dukes M.D., Romero C.C., Migliaccio K.W., and Morgan K.T. 2010. Step by Step Calculation of the Penman-Monteith Evapotranspiration (FAO-56 Method). *The Institute of Food and Agricultural Sciences (IFAS)*. AE-459

This work used eddy covariance data acquired and shared by the FLUXNET community, including these networks: AmeriFlux, AfriFlux, AsiaFlux, CarboAfrica, CarboEuropeIP, CarboItaly, CarboMont, ChinaFlux, Fluxnet-Canada, GreenGrass, ICOS, KoFlux, LBA, NECC, OzFlux-TERN, TCOS-Siberia, and USCCC. The ERA-Interim reanalysis data are provided by ECMWF and processed by LSCE. The FLUXNET eddy covariance data processing and harmonization was carried out by the European Fluxes Database Cluster, AmeriFlux Management Project, and Fluxdata project of FLUXNET, with the support of CDIAC and ICOS Ecosystem Thematic Center, and the OzFlux, ChinaFlux and AsiaFlux offices. Data from the following site IDs were used in this study: AU-How | AU-Tum | BE-Bra | BE-Vie | CA-Man | CH-Dav | DE-Geb | DE-Hai | DE-Tha | DK-Sor | DK-Za | HFI-Hyy | FI-Sod | FR-LBr | FR-Pue | IT-ColI | T-Cpz | IT-Lav | IT-Ren | IT-SRo | NL-Loo | RU-Cok | US-Ha1 | US-Los | US-Me2 | US-MMS | US-Ne1 | US-Ne2 | US-Ne3 | US-NR1 | US-PFa | US-Syv | US-Ton | US-UMB | US-Var | US-WCr.

886 **Tables**

887

Variable	Sensor	Spatial Resolution	Period	Notes
Precipitation	TRMM	0.25º	1998-2015	Huffman et al. 2010
Vegetation	MODIS	0.05º	2000-present 2002-present	Justice et al. 1998, 2002
Evapotranspiration	MODIS	0.05º	2000-present 2002-present	Mu et al. 2007
Total Water	GRACE	1.00º	2002-present	Tapley et al. 2004
Soil Moisture	GLDAS	0.25º	1979-present	Mitchell et al. 2004
Runoff	GLDAS	0.25º	1979-present	Mitchell et al. 2004

888
889
890 Table 1 List of hydrological variables and their sources used in this study
891

Basin Name	Previous studies	Total Area (km^2) Climate	Latitude of Centroid	Average annual rainfall (mm)	Average air temperature (K/C)
Amazon	Nijssen et al. 2001 Syed et al. 2005 Marengo 2005	5,084,460 Tropical Wet	6.6ºS	1800	297/24
California	Dettinger et al. 2004 Yates et al. 2009	415,254 Arid	37.5ºN	470	289/16
Colorado	Christensen et al. 2004 Christensen et al. 2007 Barnett et al. 2004	635,686 Semi-Arid	36.7ºN	160	287/14
Congo	Aerts et al. 2006 Lee et al. 2011 Tshimanga et al. 2012	3,064,930 Tropical Dry	2.5ºS	1600	298/25
Danube	Klein et al. 2012 Stagl et al. 2015 Szepszo et al. 2014	816,351 Marine	46.4ºN	728	284/11
Ganga-Brahmaputra	Roy et al. 2015 Nepal et al. 2015 Singh et al. 2006	1,525,340 Tropical Monsoon	26.9ºN	2110	296/23
Mekong	Kite, 2001 Frappart et al. 2006 Kingston et al. 2011	728,447 Tropical	18.5ºN	1275	298/25
Mississippi	Dai et al. 2009 Rodell et al. 2007 Jha et al. 2006	3,245,240 Humid Rainy	40.6ºN	765	286/13
Murray-Darling	Donohue et al. 2011 Potter et al. 2010 Pittock et al. 2011	925,029 Semi-arid	31.7ºS	350	290/17
Nile	Conway 1997 Yates et al. 1998 Elsahmy et al. 2009	2,593,050 Arid	11.9ºN	337	300/27
Yangtze	Guo et al. 2002 Xu et al. 2011 Xu et al. 2008	1,691,060 Tropical Dry	30.2ºN	1073	289/16

Table 2 River basins chosen for this study, previous water balance studies and their characteristics. The source for the precipitation and temperature is the Global Historical Climatology Network.

TRMM TMPA PRECIPITATION	Kummerow et al 1998 Huffman et al 2007 Wolff et al 2005 Amitai et al 2002 Liao et al 2009 Kummerow et al 2000 Nicholson et al 2003 Adler et al 2000 Gebremichael et al 2004
MODIS EVAPOTRANSPIRATION	Mu et al 2007 Velpuri et al 2013 Kim et al 2012 Mu et al 2011 Tang et al 2011 Gemitizi et al 2017
GLDAS NOAH RUNOFF	Rodell et al 2004 Zaichik et al 2010 Syed et al 2008

Table 3 List of previous validation studies for Evapotranspiration, Precipitation, and Runoff

Basin	R^2	Lag (months)	Avg. P	Avg. ET	Avg. SM	Avg. Runoff
Amazon	0.81	0	190.42	108.22	62.24	60.65
California	0.56	0	43.37	27.47	40.59	4.61
Colorado	0.12	-3	24.54	16.11	35.56	0.6
Congo	0.34	0	124.61	77.89	52.44	20.99
Danube	0.52	0	77.26	45.15	53.52	11.69
Ganga Brahmaputra	0.66	0	112.6	49.99	56	33.17
Mekong	0.74	1	135.46	86.71	53.88	22.72
Mississippi	0.17	0	71.7	42.43	44.02	7.19
Murray Darling	0.13	0	40.31	23.07	35.25	0.9
Nile	0.37	0	54.79	38.29	45.79	5.42
Yangtze	0.36	1	86.92	57.26	67.22	22.72

Table 4 Maximum Correlation between monthly P-ET-R and the GRACE Water Equivalent Thickness Anomaly and the corresponding lag (for the maximum correlation), and the average values for precipitation, evapotranspiration, soil moisture and runoff in mm. All of the R^2 values are significant at the p=0.05 level.

Basin	R^2	Lag (months)	Avg. P	Avg. ET	Avg. SM	Avg. Runoff
Amazon	0.81	0	190.42	108.22	62.24	60.65
California	0.56	0	43.37	27.47	40.59	4.61
Colorado	0.12	-3	24.54	16.11	35.56	0.6
Congo	0.34	0	124.61	77.89	52.44	20.99
Danube	0.52	0	77.26	45.15	53.52	11.69
Ganga Brahmaputra	0.66	0	112.6	49.99	56	33.17
Mekong	0.74	1	135.46	86.71	53.88	22.72
Mississippi	0.17	0	71.7	42.43	44.02	7.19
Murray Darling	0.13	0	40.31	23.07	35.25	0.9
Nile	0.37	0	54.79	38.29	45.79	5.42
Yangtze	0.36	1	86.92	57.26	67.22	22.72

Table 4 Maximum Correlation between monthly P-ET-R and the GRACE Water Equivalent Thickness Anomaly and the corresponding lag (for the maximum correlation), and the average values for precipitation, evapotranspiration, soil moisture and runoff in mm. All of the R^2 values are significant at the p=0.05 level.

916
917

	Precipitation	NDVI	LST	ET	Runoff	Soil Moisture	Total Water
Amazon	-0.4 /0.61 /0	-0.04 /0.08 /0	0/0 /0	-0.17/0.29 /0	-0.66/2.6 /-0.1	-0.39/0.23 /-0.3	-28/30.4 /0
California	-0.92 / 3.47 /-0.06	-0.17/0.22 /0	-0.02/0.02 /0	-0.34/0.47 /0	-0.86/2.33 /0.01	-0.37/0.24 /-0.02	-17.8/19.5 /-1.51
Colorado	-0.93/ 2.18 /-0.03	-0.25/0.3 /0	-0.02/0.02 /0	-0.42/0.76 /0	-0.78/2.72 /-0.08	-0.38/0.18 /-0.03	-8.9/7.4 /-0.96
Congo	-0.46/ 1.58 /0	-0.05/0.05 /0	0/0 /0	-0.38/0.86 /0	-0.85/3.22 /-0.15	-0.41/0.27 /-0.03	-10.5/13.6 /-0.81
Danube	-0.94/1.15 /0.01	-0.58/0.44 /0	-0.03/0.02 /0	-0.24/0.2 /0	-0.78/1.85 /-0.03	-0.44/0.24 /-0.2	-16.7/17.5 /-0.03
Ganga Brahmaputra	-0.83/ 2.27 /0	-0.13/0.22 /0	-0.01/0.01 /0	-0.44/0.72 /0	-0.56/1.44 /-0.05	-0.41/0.15 /-0.03	-20.8/27 /-1.51
Mekong	-0.84/ 2.06 /-0.02	-0.09/0.09 /0	-0.01/0.01 /0	-0.19/0.21 /0	-0.83/9.2 /-0.26	-0.42/0.68 /-0.04	-28.3/36.5 /0.98
Mississippi	-0.58/0.82 /-0.01	-0.27/0.27 /0	-0.02/0.02 /0	-0.3/0.25 /0	-0.76/1.52 /-0.02	-0.46/0.15 /-0.03	-12.7/12.3 /0.02
Murray Darling	-0.95/ 1.73 /-0.06	-0.23/0.38 /-0.01	-0.03/0.02 /0	-0.63/1.7 /0	-0.83/3.04 /-0.05	-0.41/0.43 /-0.03	-5.5/17.1 /3.23
Nile	-0.76/ 4.73 /-0.04	-0.07/0.1 /0	-0.01/0.01 /0	-0.62/2.23 /0.01	-0.63/5.44 /-0.21	-0.37/0.34 /-0.04	-7.9/9.3 /0.22
Yangtze	-0.61/ 0.95 /-0.01	-0.16/0.1 /0	-0.01/0.01 /0	-0.12/0.12 /0	-0.61/2.91 /-0.12	-0.36/0.17 /-0.03	-9.2/13.3 /0.41

918
919 Table 5 Range of anomaly index (min/max/mean) for hydrological variables for major global
920 river basins. These correspond to basin averaged monthly values. The reported values are
921 maximum, minimum and mean anomaly index. The anomaly index (dimensionless) is defined as
922 the monthly anomaly divided by the monthly climatology
923

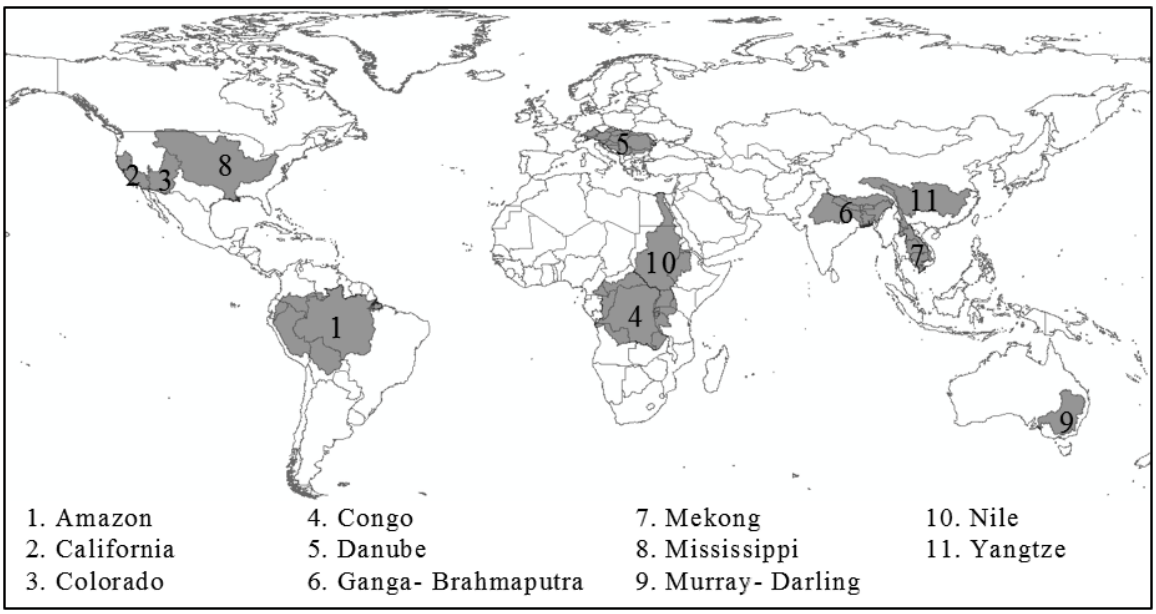

Figure 1 Map showing the major global river basins studied in this paper. Basin shapes are extracted from the Food and Agricultural Organization of the United Nations (FAO-UN), Major Hydrological Basins shapefile.

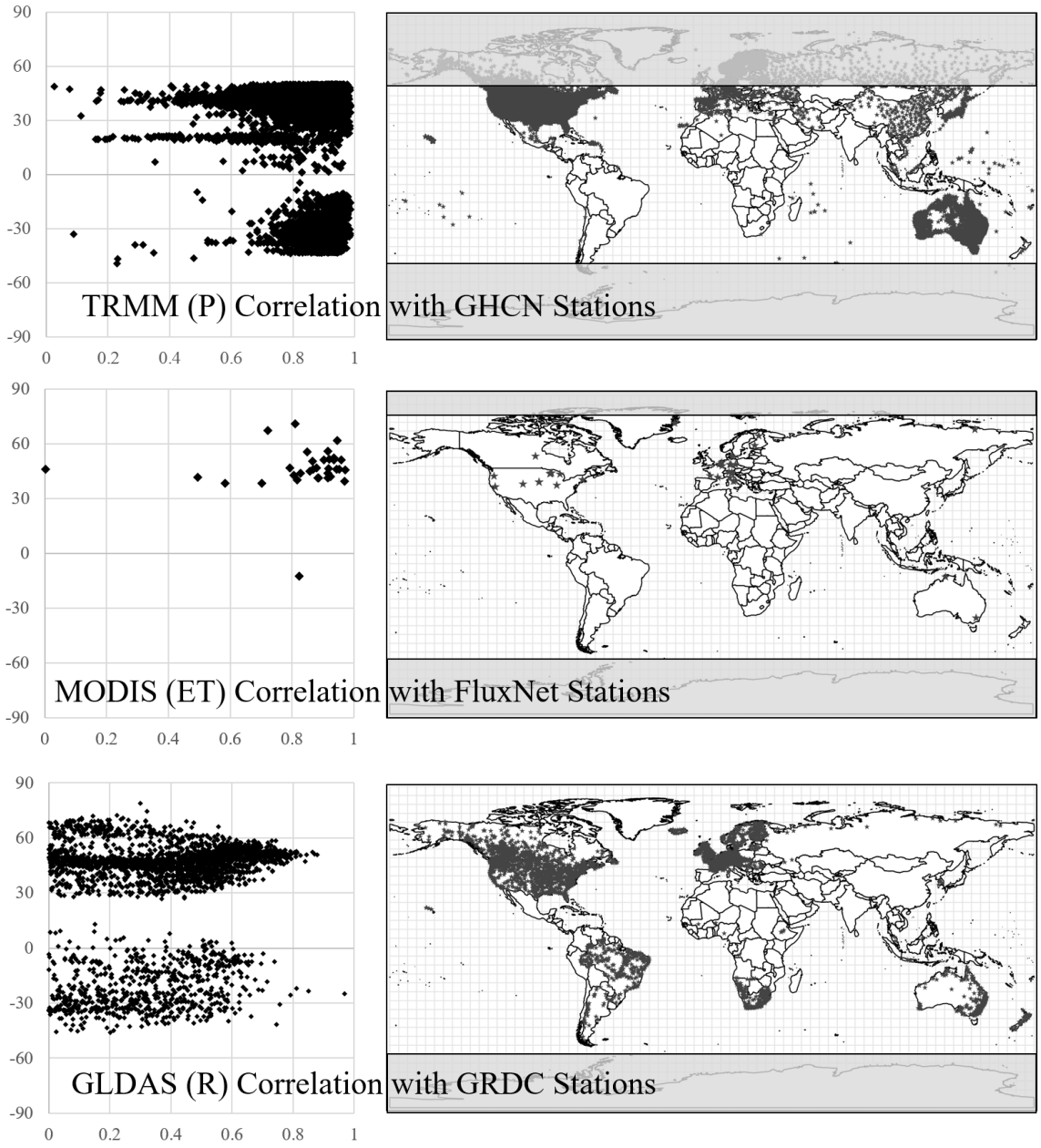

Figure 2 Ground Station Data is correlated with Satellite and Modeled parameters from TRMM Precipitation, MODIS Evapotranspiration, and GLDAS-NOAH Runoff, the correlation values are plotted by latitude to demonstrate the variation in satellite performance and the availability of in-situ measurements in the northern and southern hemispheres. The high latitude regions are greyed where satellite and model data is not produced.

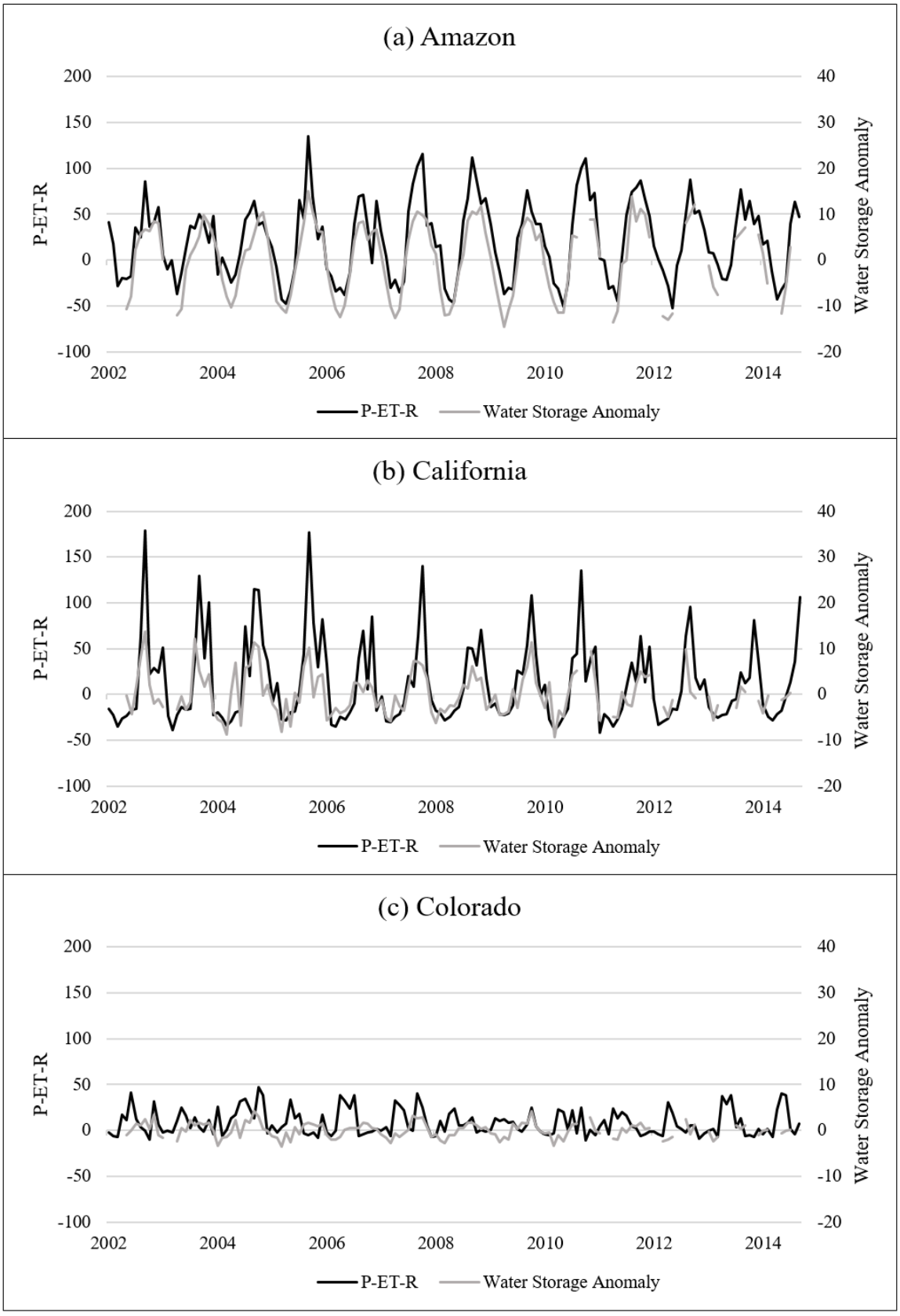
(a) Amazon
P-ET-R
Water Storage Anomaly
200
150
100
50
0
-50
-100
40
30
20
10
0
-10
-20
2002
2004
2006
2008
2010
2012
2014
P-ET-R
Water Storage Anomaly
(b) California
P-ET-R
Water Storage Anomaly
P-ET-R
Water Storage Anomaly
(c) Colorado
P-ET-R
Water Storage Anomaly
P-ET-R
Water Storage Anomaly

940

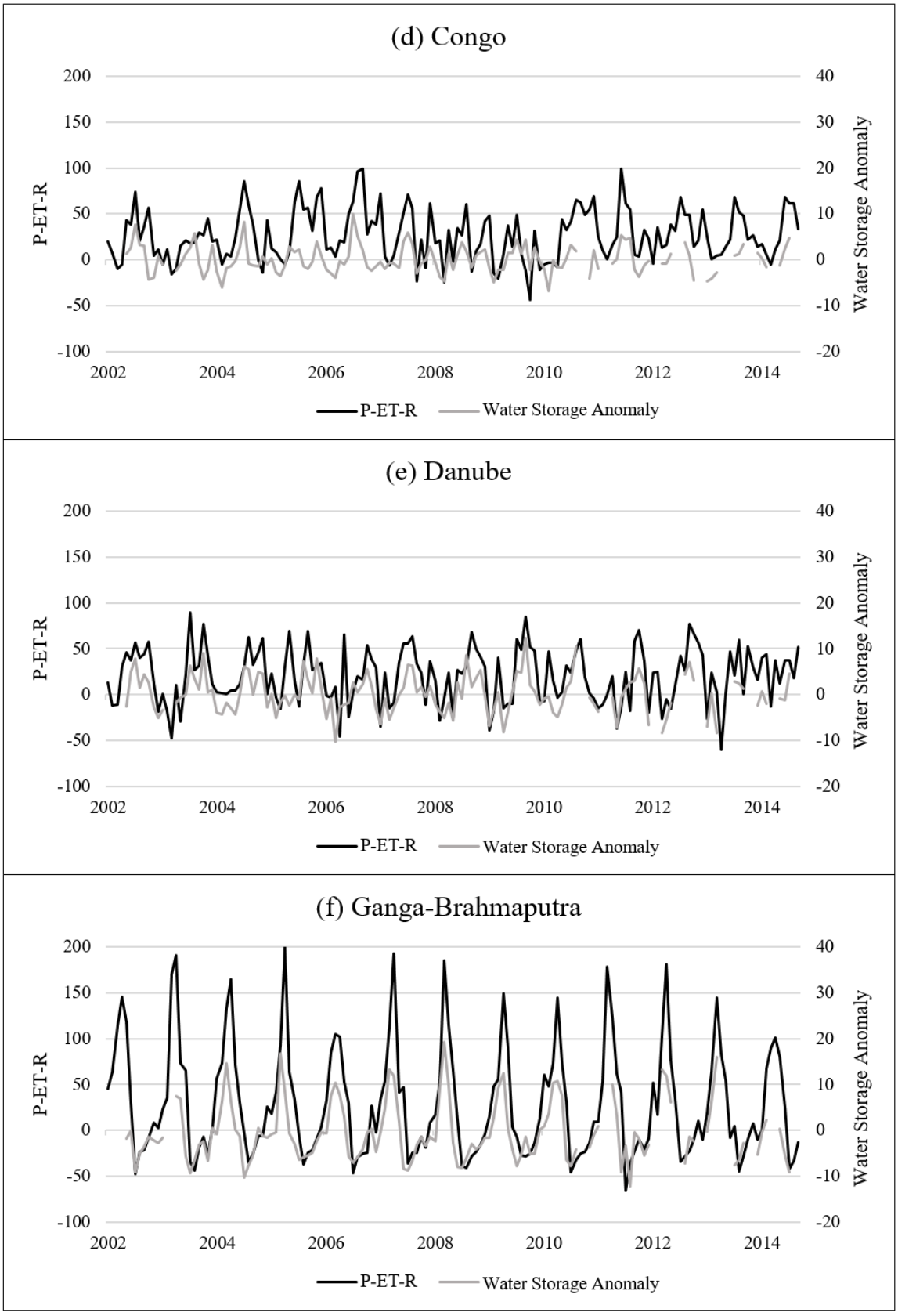
(d) Congo
200
150
100
50
0
-50
-100
40
30
20
10
0
-10
-20
2002
2004
2006
2008
2010
2012
2014
P-ET-R
Water Storage Anomaly
P-ET-R
Water Storage Anomaly
(e) Danube
200
150
100
50
0
-50
-100
40
30
20
10
0
-10
-20
2002
2004
2006
2008
2010
2012
2014
P-ET-R
Water Storage Anomaly
P-ET-R
Water Storage Anomaly
(f) Ganga-Brahmaputra
200
150
100
50
0
-50
-100
40
30
20
10
0
-10
-20
2002
2004
2006
2008
2010
2012
2014
P-ET-R
Water Storage Anomaly
P-ET-R
Water Storage Anomaly

941

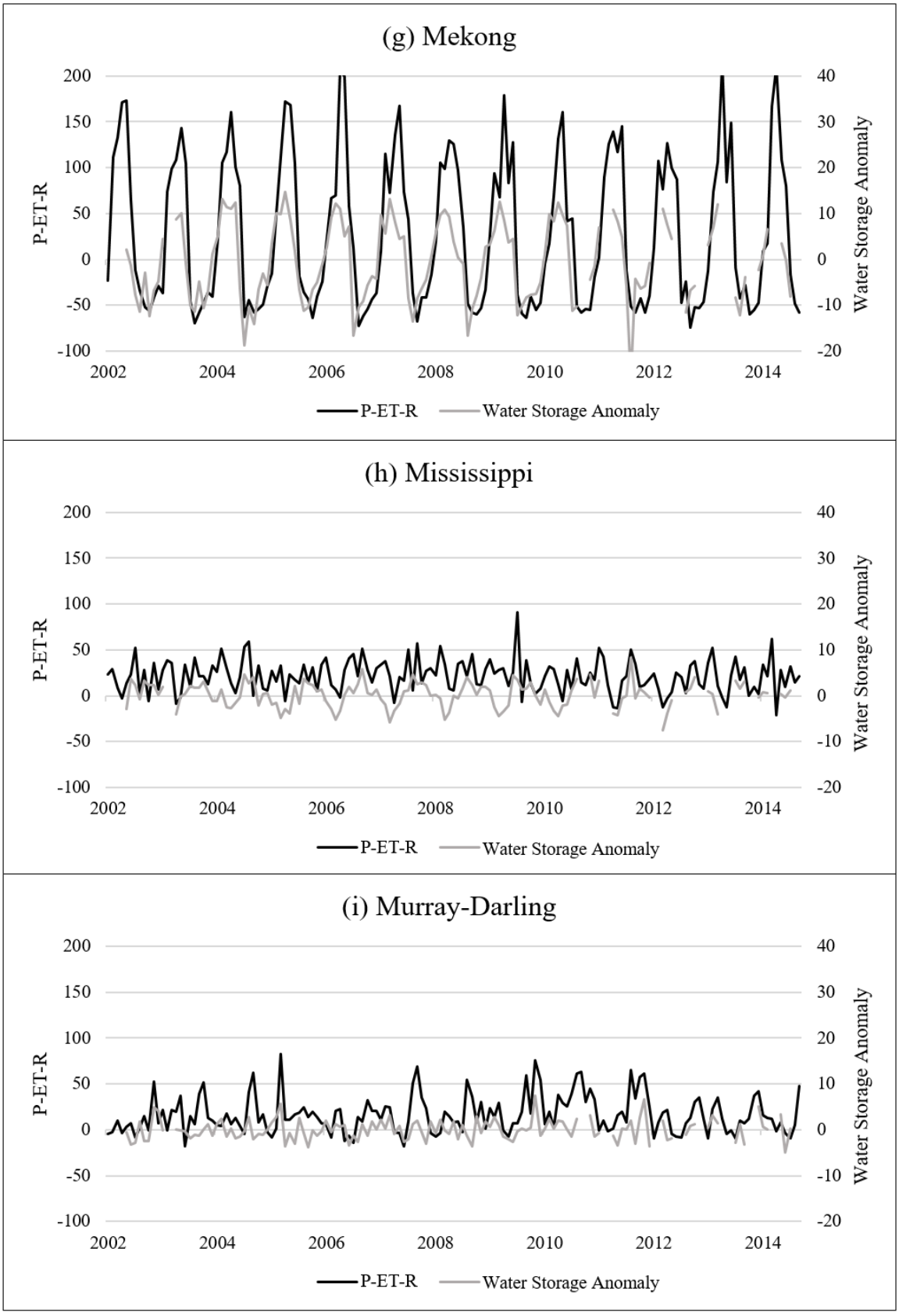
(g) Mekong
P-ET-R
Water Storage Anomaly
200
150
100
50
0
-50
-100
40
30
20
10
0
-10
-20
2002
2004
2006
2008
2010
2012
2014
P-ET-R
Water Storage Anomaly
(h) Mississippi
P-ET-R
Water Storage Anomaly
200
150
100
50
0
-50
-100
40
30
20
10
0
-10
-20
2002
2004
2006
2008
2010
2012
2014
P-ET-R
Water Storage Anomaly
(i) Murray-Darling
P-ET-R
Water Storage Anomaly
200
150
100
50
0
-50
-100
40
30
20
10
0
-10
-20
2002
2004
2006
2008
2010
2012
2014
P-ET-R
Water Storage Anomaly

942
943

944

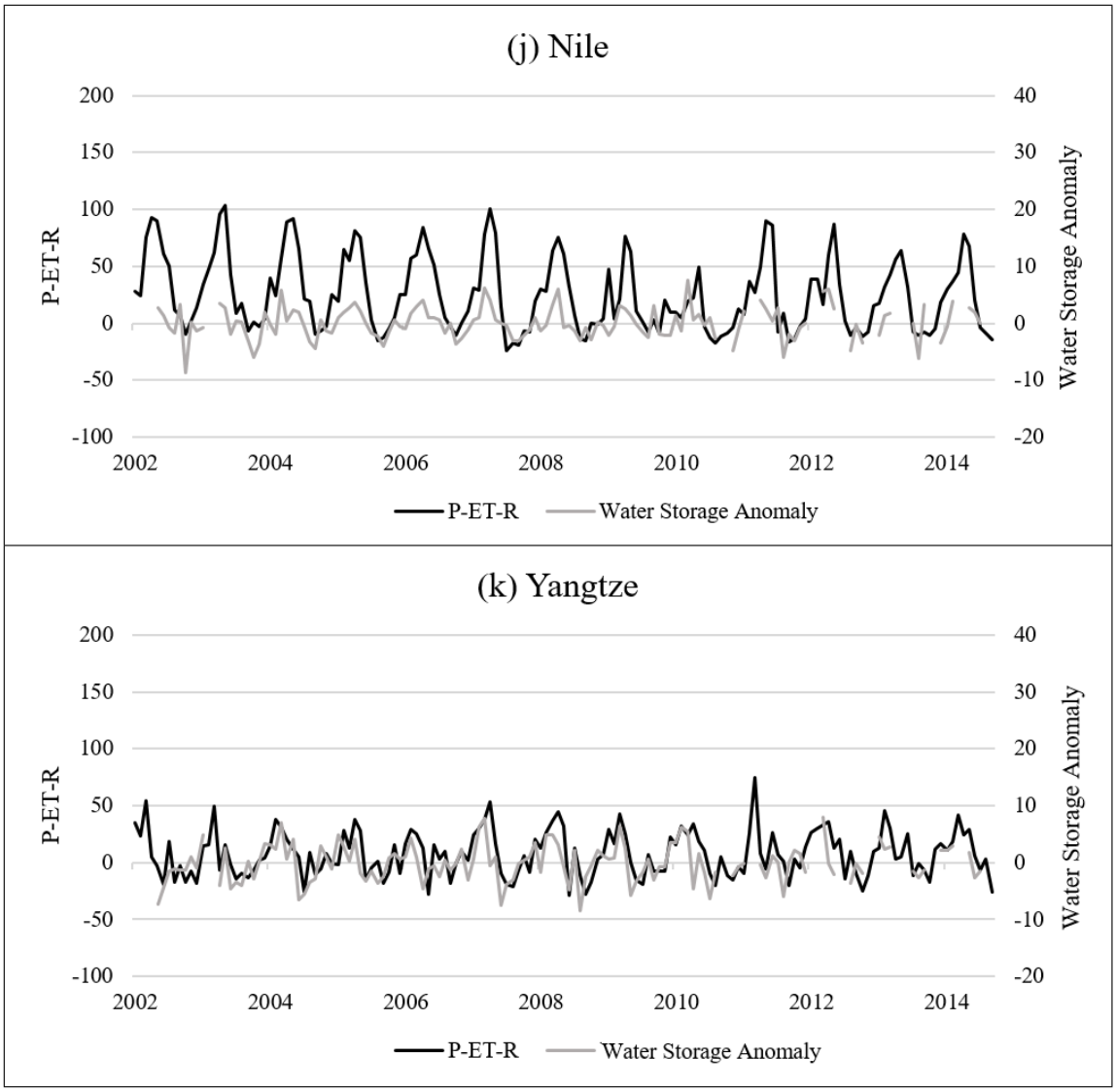

945
946
947 Figure 3a Precipitation-ET—Runoff (P-ET-R) and GRACE water equivalent thickness
948 anomalies (Water Storage) for the major river basins of the world (a) Amazon (b) California (c)
949 Colorado (d) Congo (e) Danube (f) Ganga-Brahmaputra (g) Mekong (h) Mississippi (i) Murray-
950 Darling (j) Nile (k) Yangtze River basins.
951

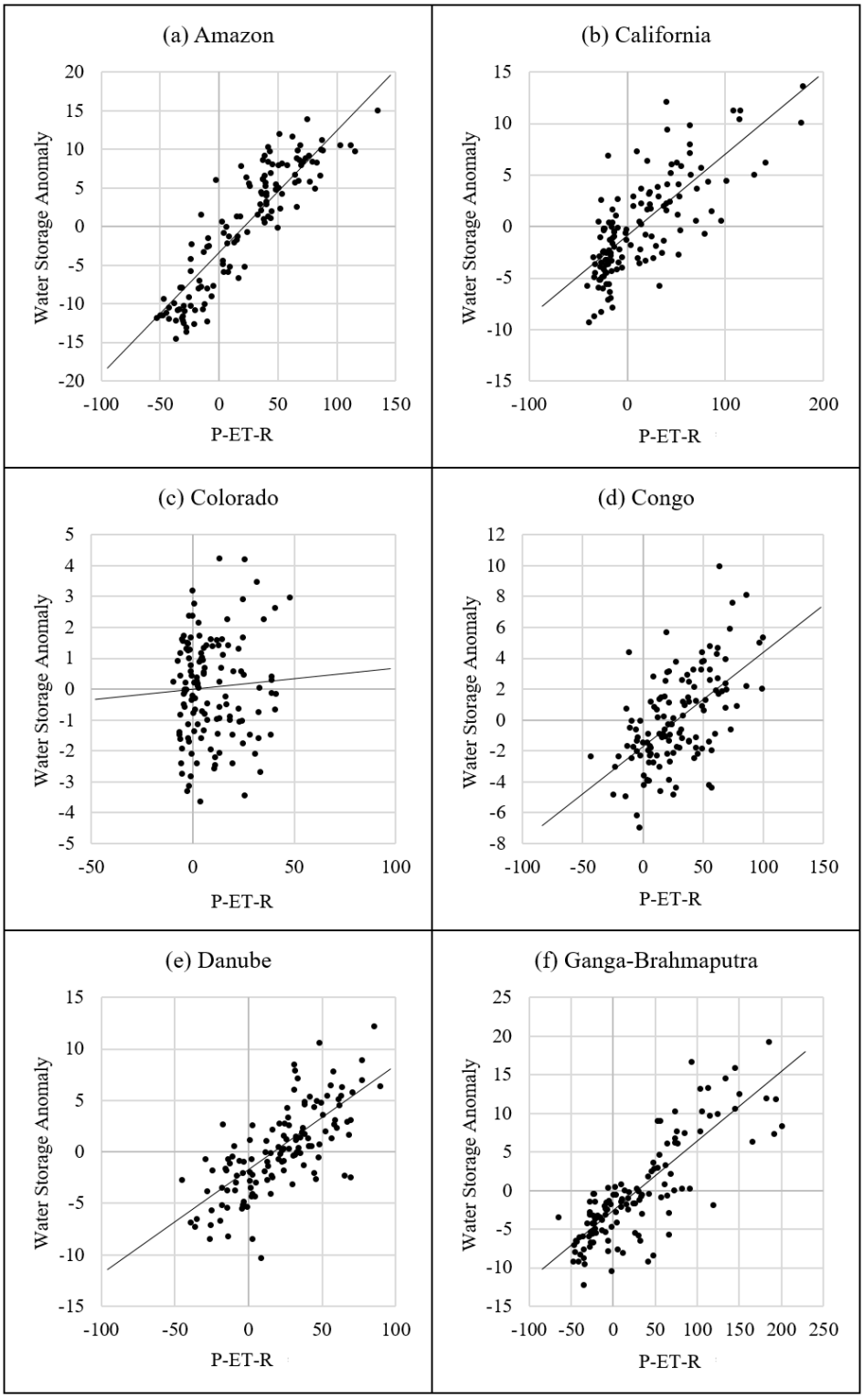
(a) Amazon
Water Storage Anomaly
P-ET-R
(b) California
Water Storage Anomaly
P-ET-R
(c) Colorado
Water Storage Anomaly
P-ET-R
(d) Congo
Water Storage Anomaly
P-ET-R
(e) Danube
Water Storage Anomaly
P-ET-R
(f) Ganga-Brahmaputra
Water Storage Anomaly
P-ET-R

952

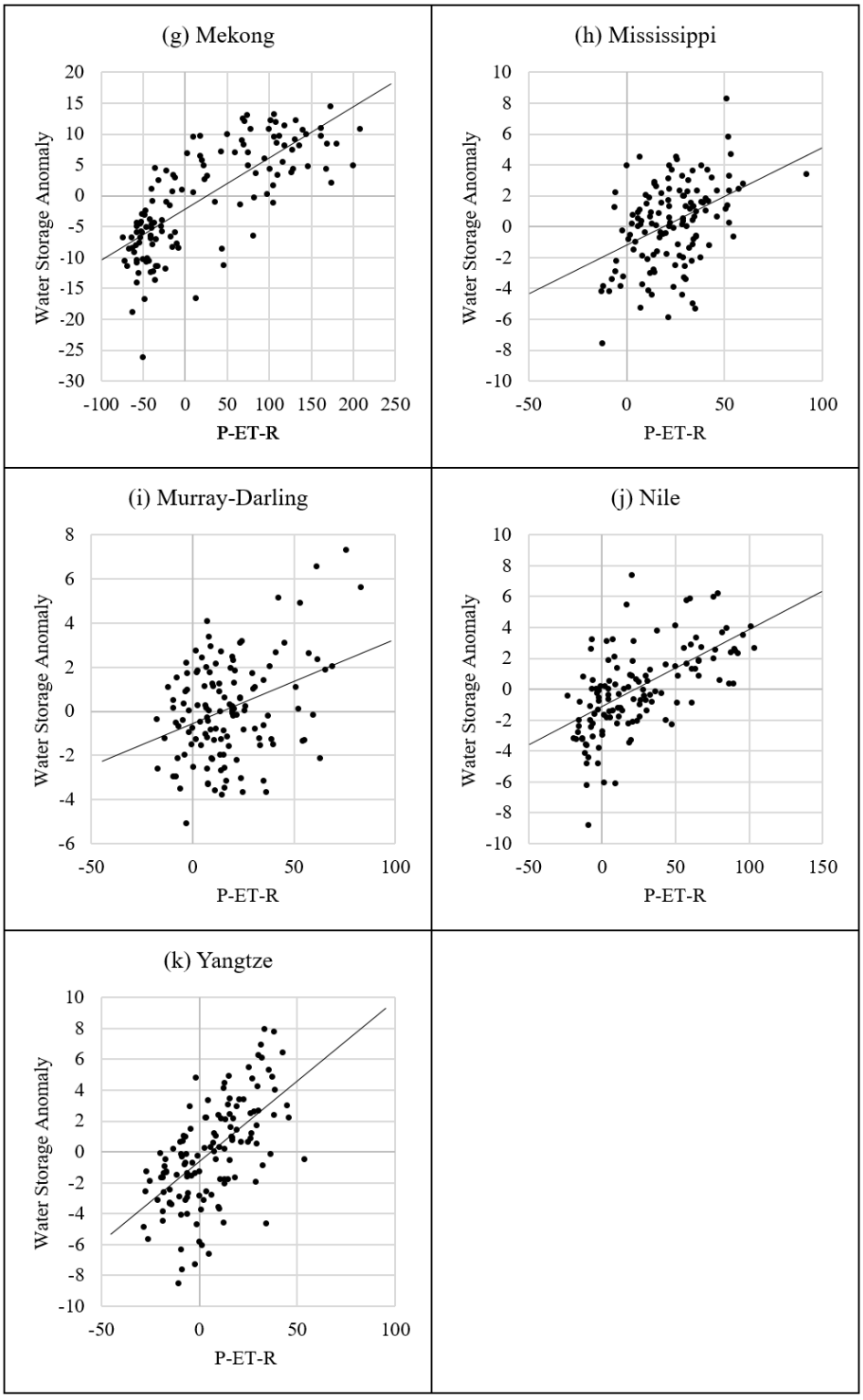

Figure 3b Scatterplots of the Precipitation-ET—Runoff (P-ET-R) compared with GRACE Water Storage Anomalies for (a) Amazon (b) California (c) Colorado (d) Congo (e) Danube (f) Ganga-Brahmaputra (g) Mekong (h) Mississippi (i) Murray-Darling (j) Nile (k) Yangtze River basins.

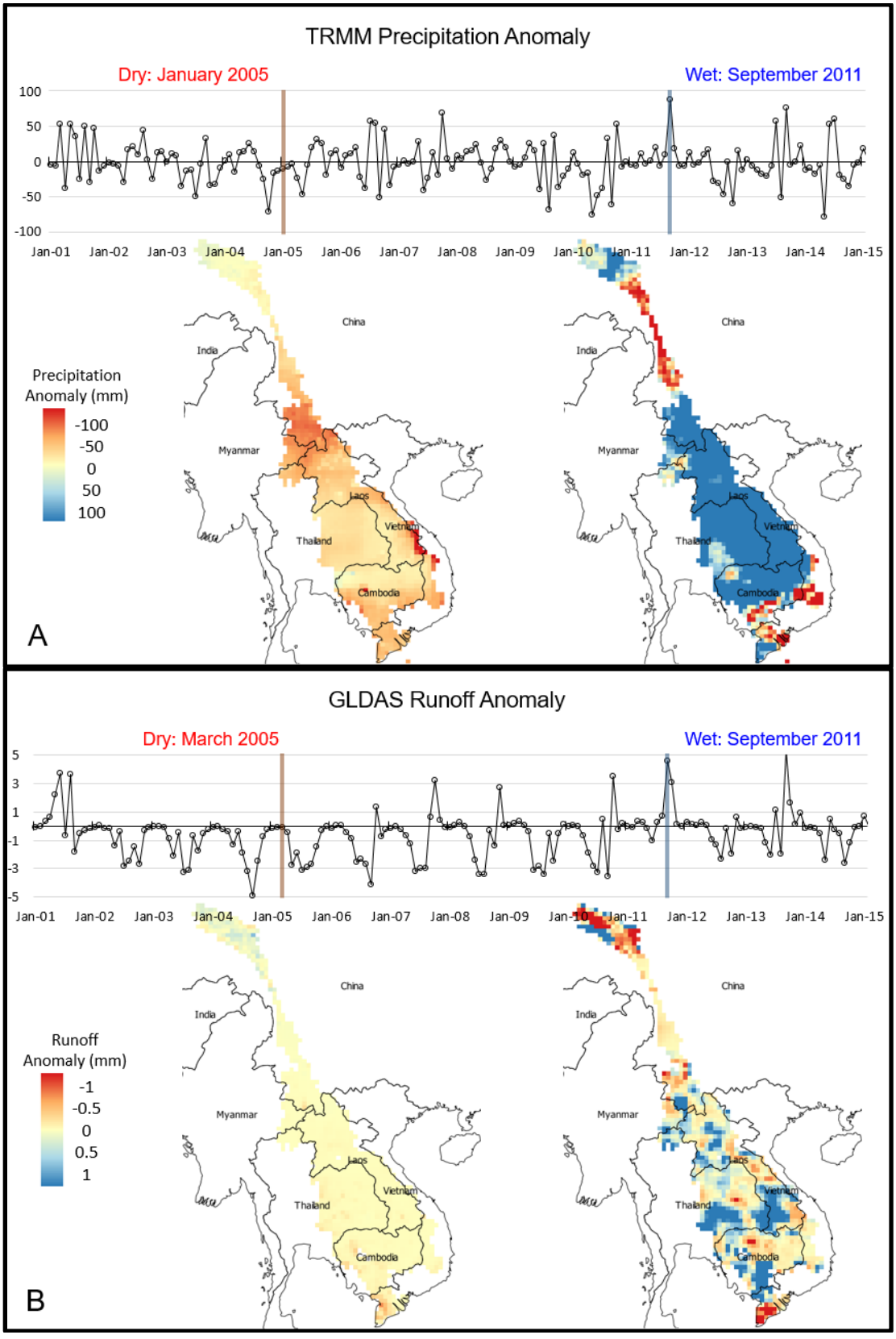
TRMM Precipitation Anomaly
Dry: January 2005
Wet: September 2011
100
50
0
-50
-100
Jan-01
Jan-02
Jan-03
Jan-04
Jan-05
Jan-06
Jan-07
Jan-08
Jan-09
Jan-10
Jan-11
Jan-12
Jan-13
Jan-14
Jan-15
Precipitation Anomaly (mm)
-100
-50
0
50
100
China
India
Myanmar
Laos
Vietnam
Thailand
Cambodia
A
GLDAS Runoff Anomaly
Dry: March 2005
Wet: September 2011
5
3
1
-1
-3
-5
Runoff Anomaly (mm)
-1
-0.5
0
0.5
1
B

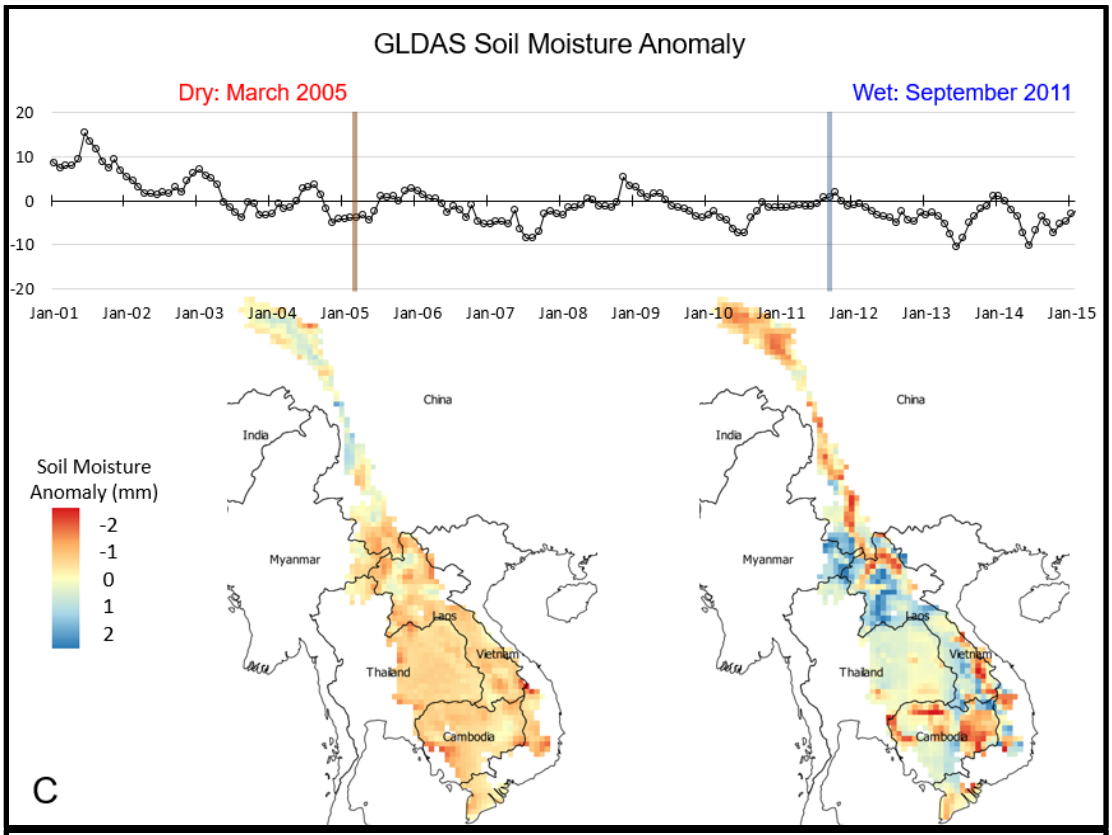
GLDAS Soil Moisture Anomaly
Dry: March 2005
Wet: September 2011
20
10
0
-10
-20
Jan-01
Jan-02
Jan-03
Jan-04
Jan-05
Jan-06
Jan-07
Jan-08
Jan-09
Jan-10
Jan-11
Jan-12
Jan-13
Jan-14
Jan-15
Soil Moisture Anomaly (mm)
-2
-1
0
1
2
China
India
Myanmar
Laos
Vietnam
Thailand
Cambodia
C

963

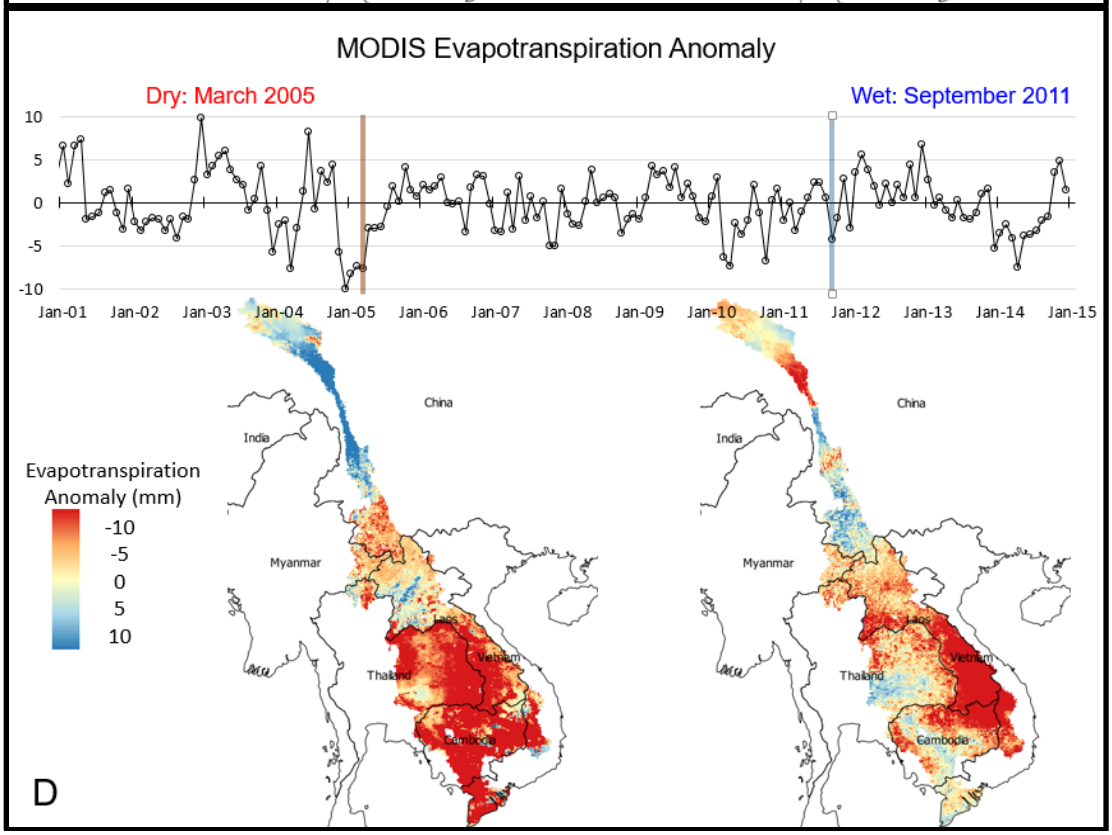
MODIS Evapotranspiration Anomaly
Dry: March 2005
Wet: September 2011
10
5
0
-5
-10
Jan-01
Jan-02
Jan-03
Jan-04
Jan-05
Jan-06
Jan-07
Jan-08
Jan-09
Jan-10
Jan-11
Jan-12
Jan-13
Jan-14
Jan-15
Evapotranspiration Anomaly (mm)
-10
-5
0
5
10
China
India
Myanmar
Laos
Vietnam
Thailand
Cambodia
D

964

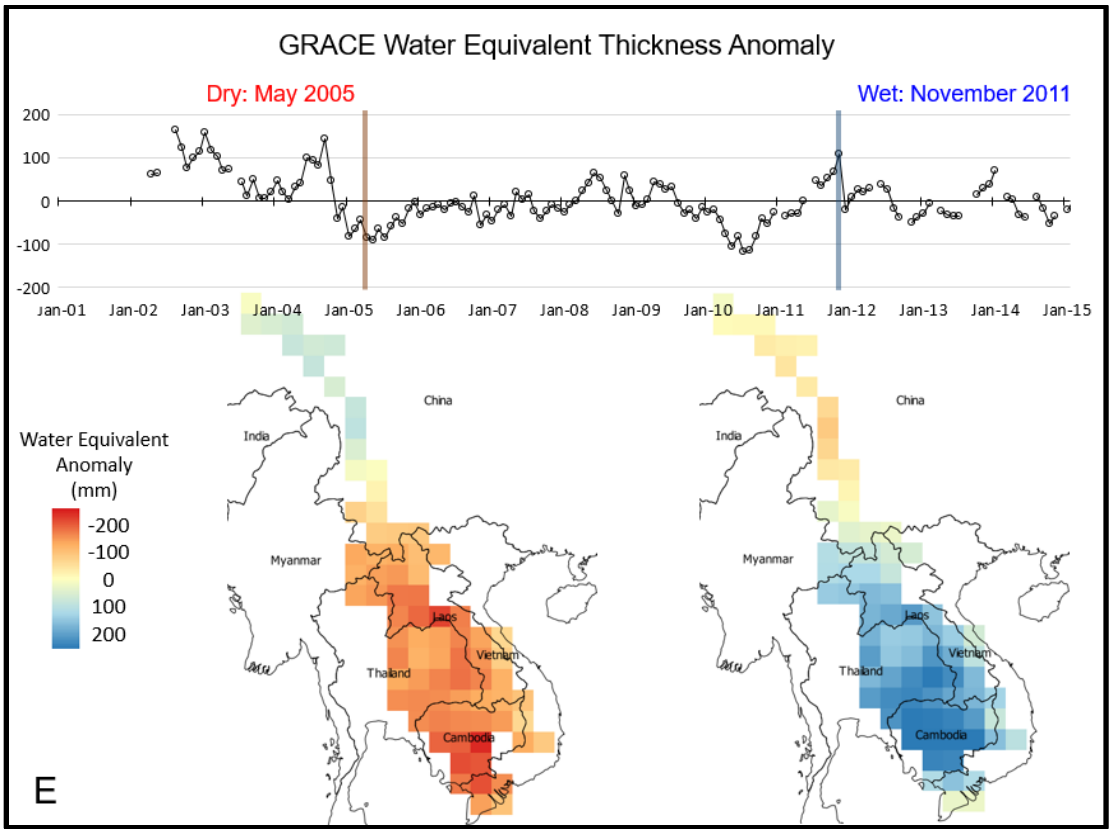

Figure 4 Mekong River Basin Time Series of (a) TRMM Precipitation Anomaly, (b) GLDAS Runoff Anomaly, (c) GLDAS Soil Moisture Anomaly, (d) MODIS ET anomaly and (e) GRACE Water Equivalent Thickness Anomaly and maps for identified wet and dry months

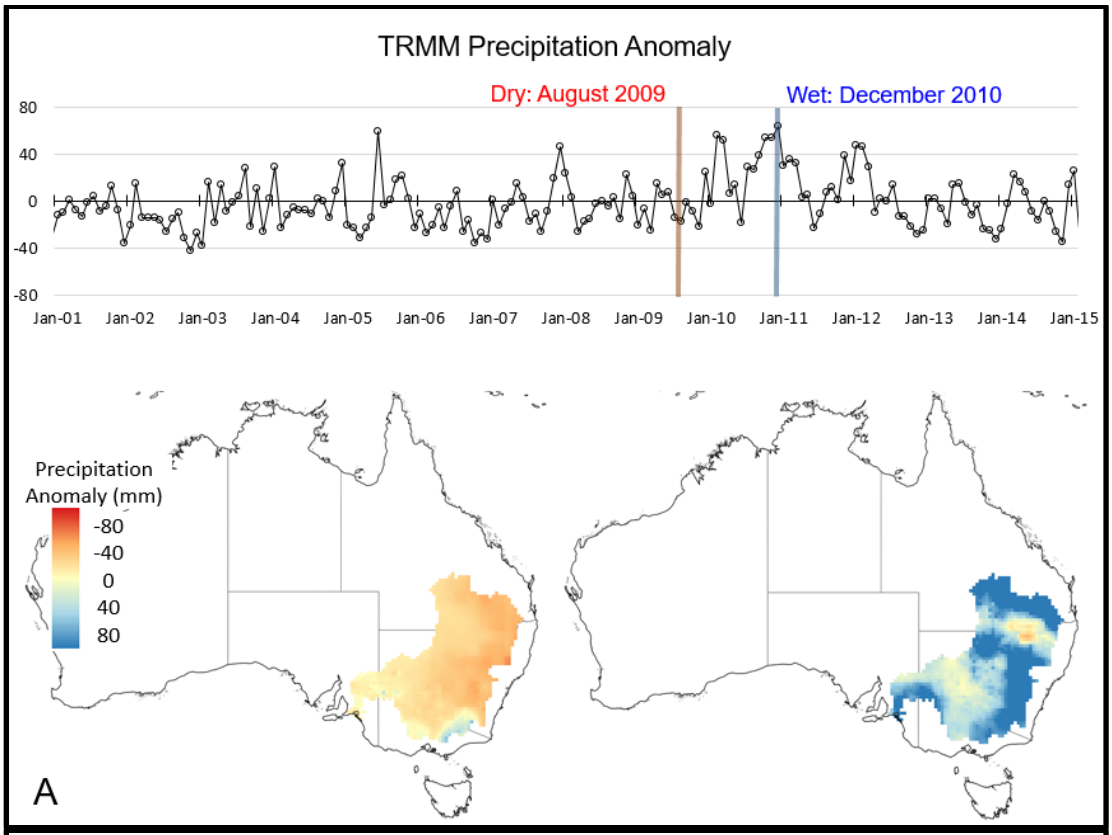
TRMM Precipitation Anomaly
Dry: August 2009
Wet: December 2010
80
40
0
-40
-80
Jan-01 Jan-02 Jan-03 Jan-04 Jan-05 Jan-06 Jan-07 Jan-08 Jan-09 Jan-10 Jan-11 Jan-12 Jan-13 Jan-14 Jan-15
Precipitation Anomaly (mm)
-80
-40
0
40
80
A

971

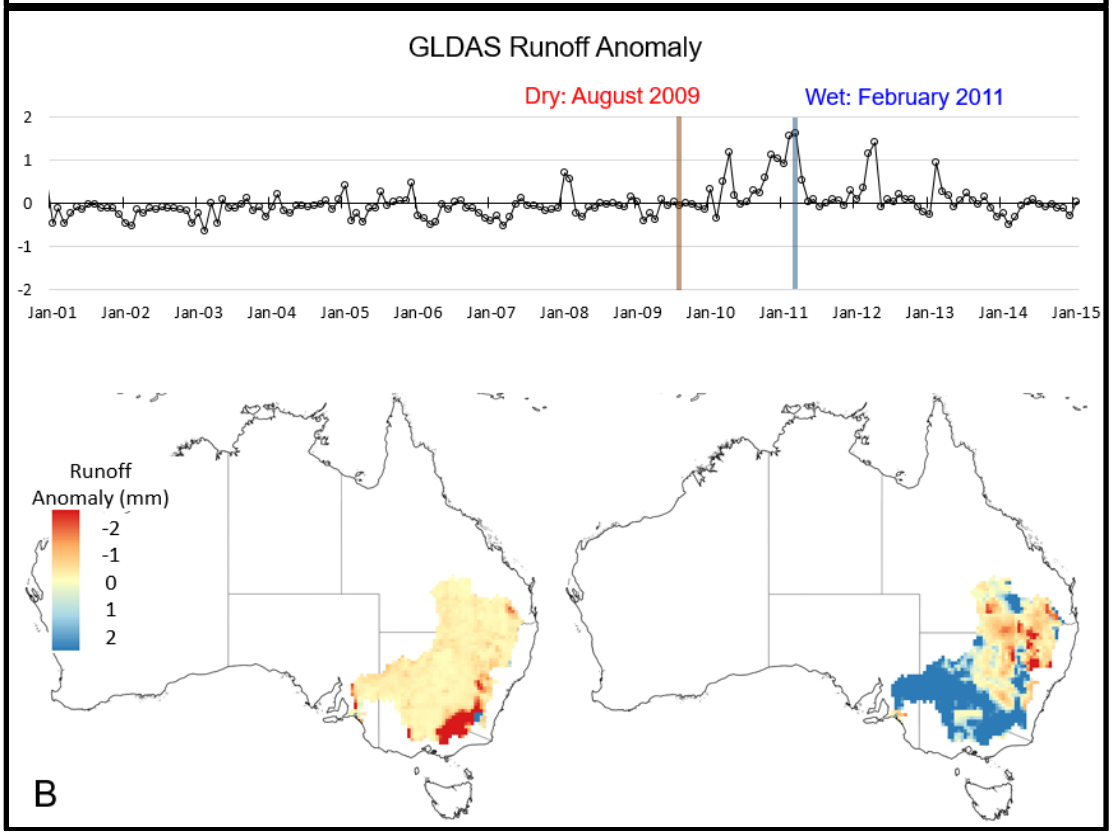
GLDAS Runoff Anomaly
Dry: August 2009
Wet: February 2011
2
1
0
-1
-2
Jan-01 Jan-02 Jan-03 Jan-04 Jan-05 Jan-06 Jan-07 Jan-08 Jan-09 Jan-10 Jan-11 Jan-12 Jan-13 Jan-14 Jan-15
Runoff Anomaly (mm)
-2
-1
0
1
2
B

972

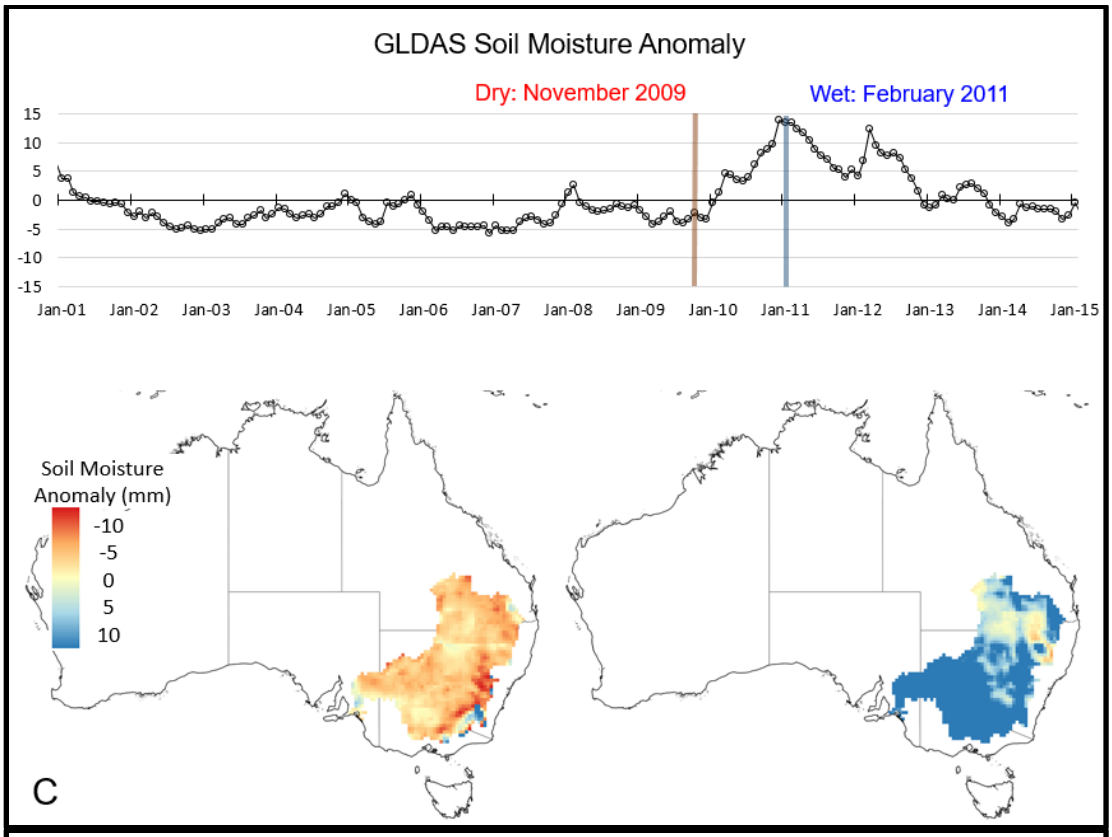
GLDAS Soil Moisture Anomaly
Dry: November 2009
Wet: February 2011
15
10
5
0
-5
-10
-15
Jan-01
Jan-02
Jan-03
Jan-04
Jan-05
Jan-06
Jan-07
Jan-08
Jan-09
Jan-10
Jan-11
Jan-12
Jan-13
Jan-14
Jan-15
Soil Moisture Anomaly (mm)
-10
-5
0
5
10
C

973

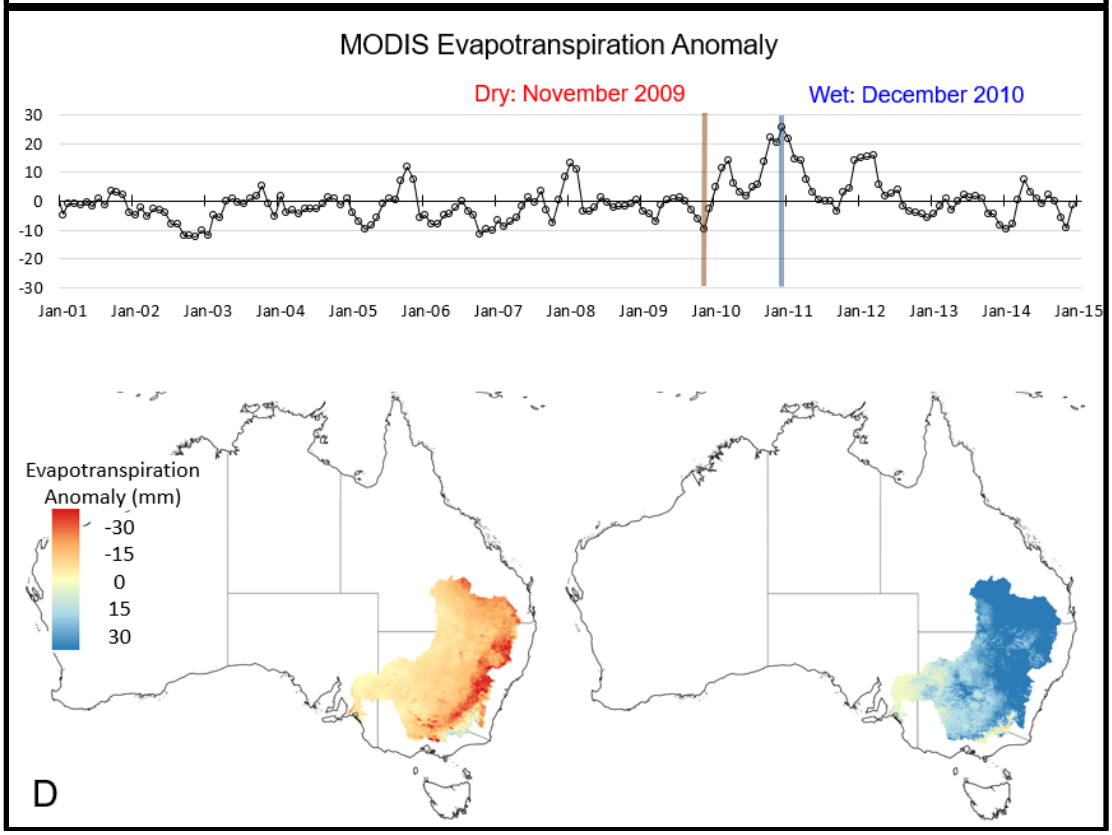
MODIS Evapotranspiration Anomaly
Dry: November 2009
Wet: December 2010
30
20
10
0
-10
-20
-30
Jan-01
Jan-02
Jan-03
Jan-04
Jan-05
Jan-06
Jan-07
Jan-08
Jan-09
Jan-10
Jan-11
Jan-12
Jan-13
Jan-14
Jan-15
Evapotranspiration Anomaly (mm)
-30
-15
0
15
30
D

974
975

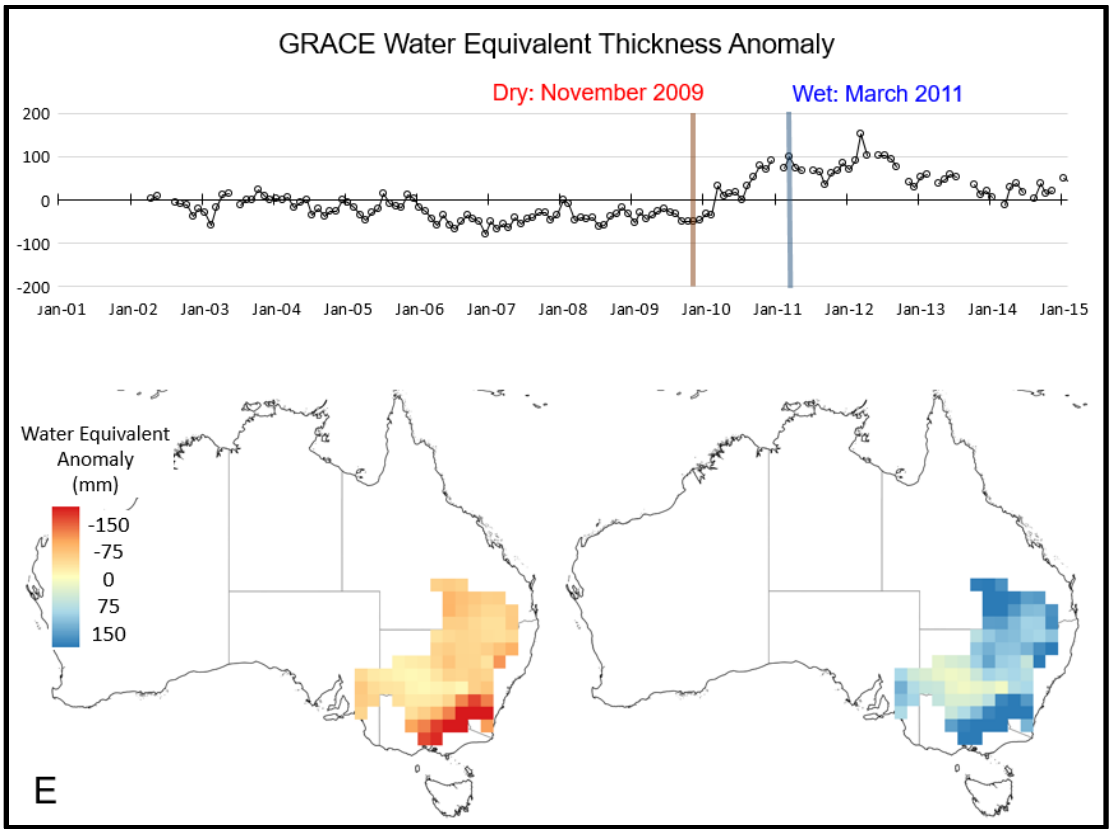

Figure 5 Murray-Darling River Basin Time Series of (a) TRMM Precipitation Anomaly, (b) GLDAS Runoff Anomaly, (c) GLDAS Soil Moisture Anomaly, (d) MODIS ET anomaly and (e) GRACE Water Equivalent Thickness Anomaly and maps for identified wet and dry months

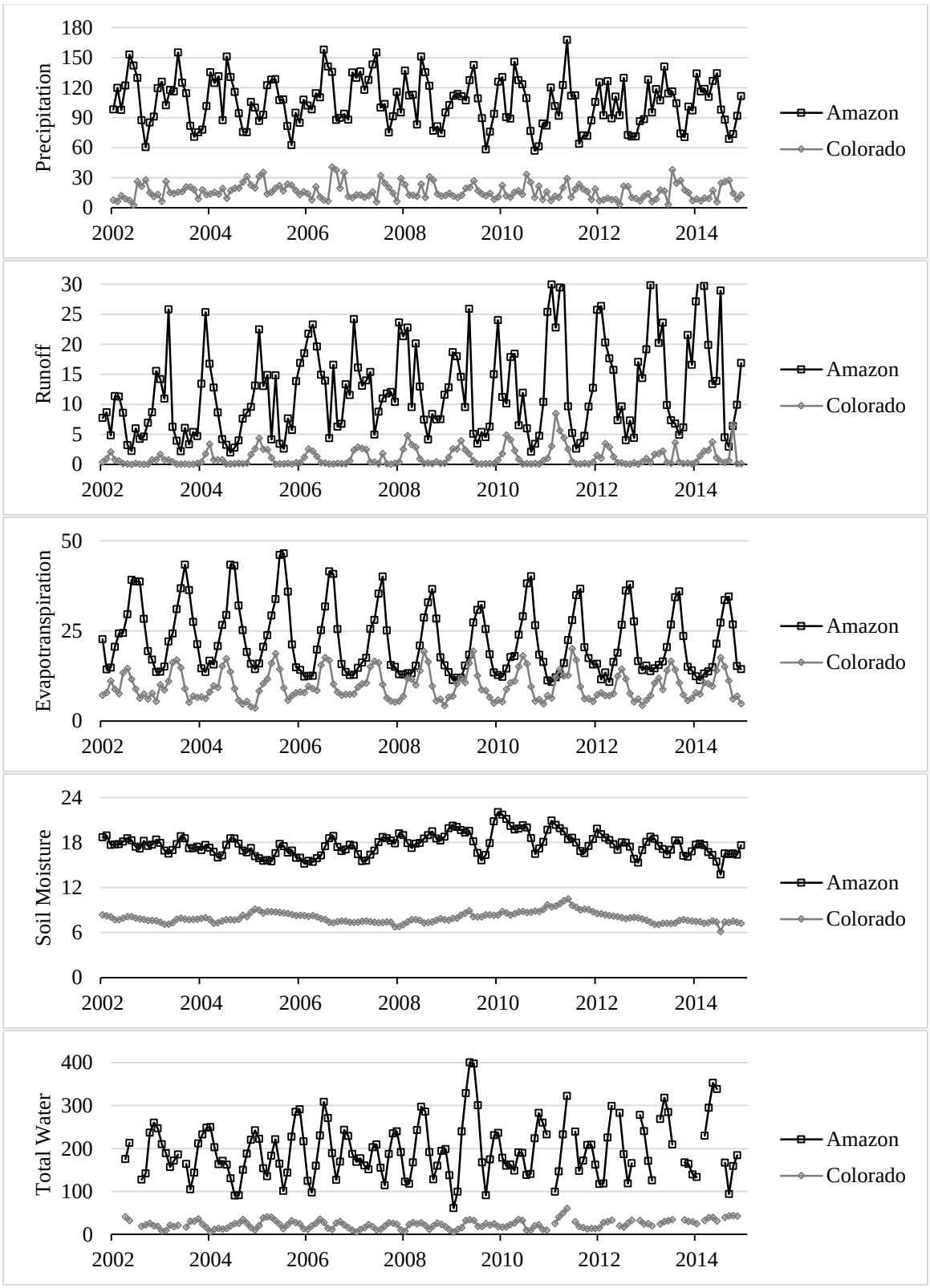

Figure 6 The spatial standard deviation of precipitation, runoff, ET, soil moisture and total water (all in mm) for the Amazon and Colorado River Basin

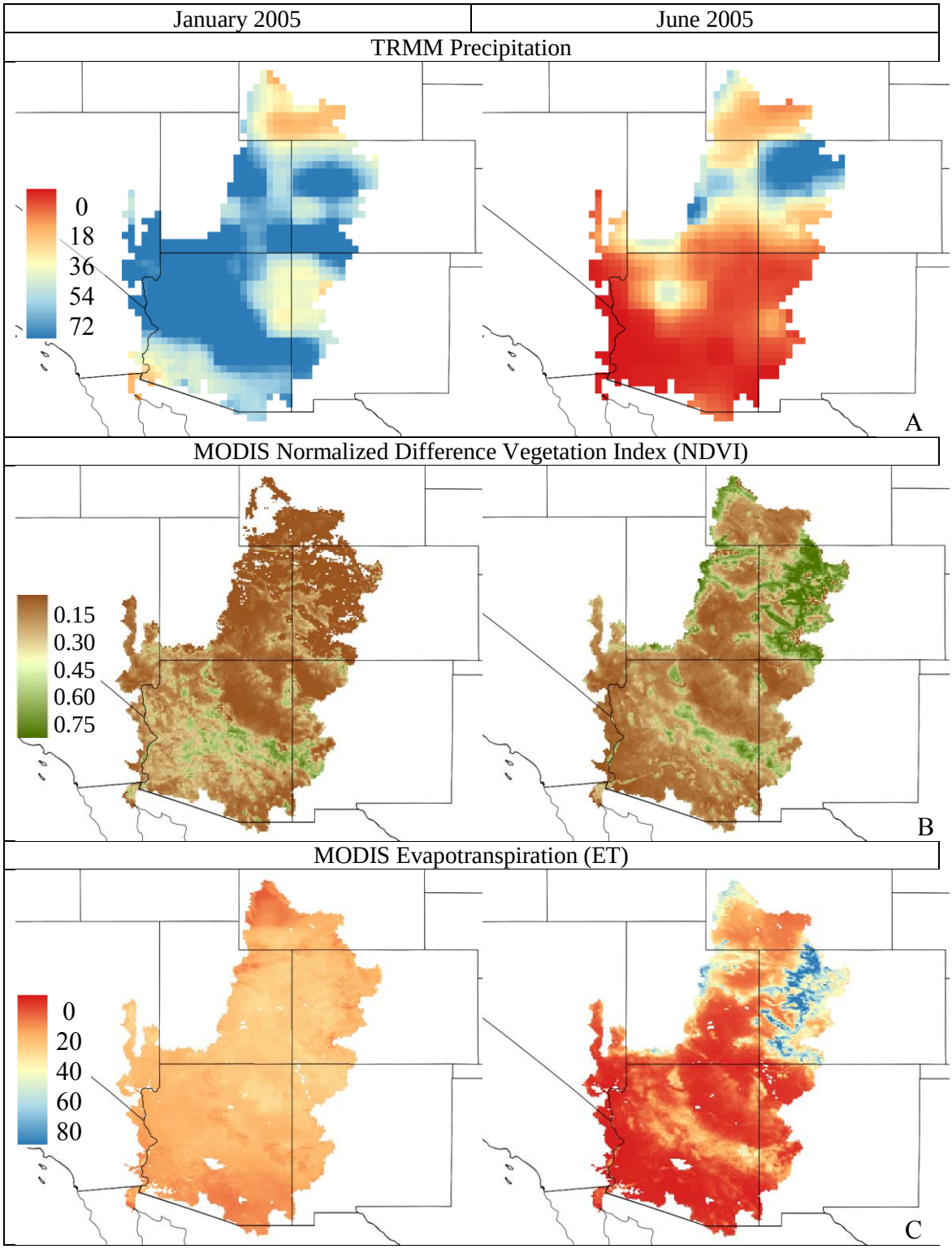

Figure 7 Monthly spatial variations of (a) Precipitation, (b) NDVI, and (c) ET (in mm) for the Colorado River basin for January 2005 and June 2005

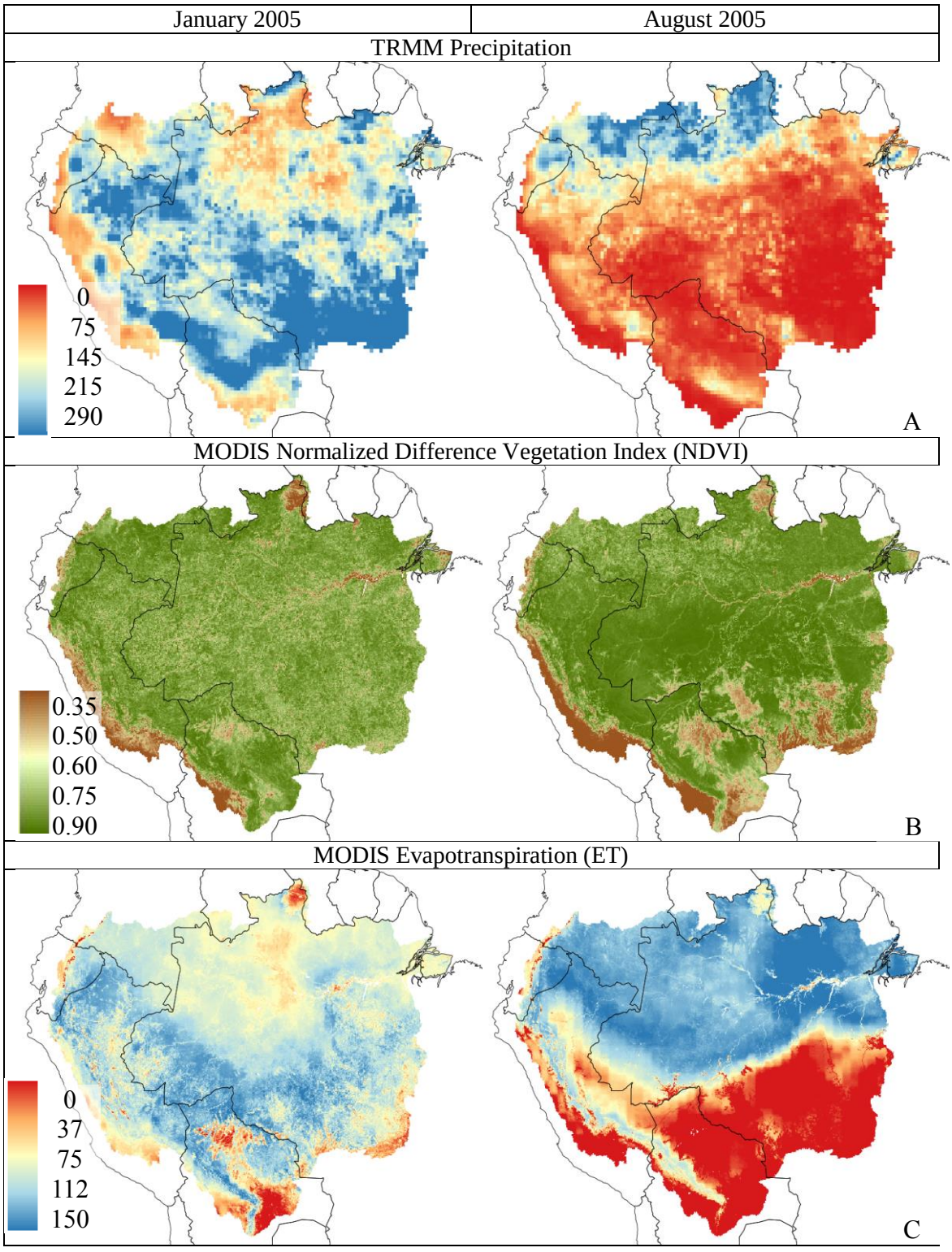

Figure 8 Monthly spatial variations of (a) Precipitation, (b) NDVI, and (c) ET (in mm) for the Amazon River basin for January 2005 and August 2005

998

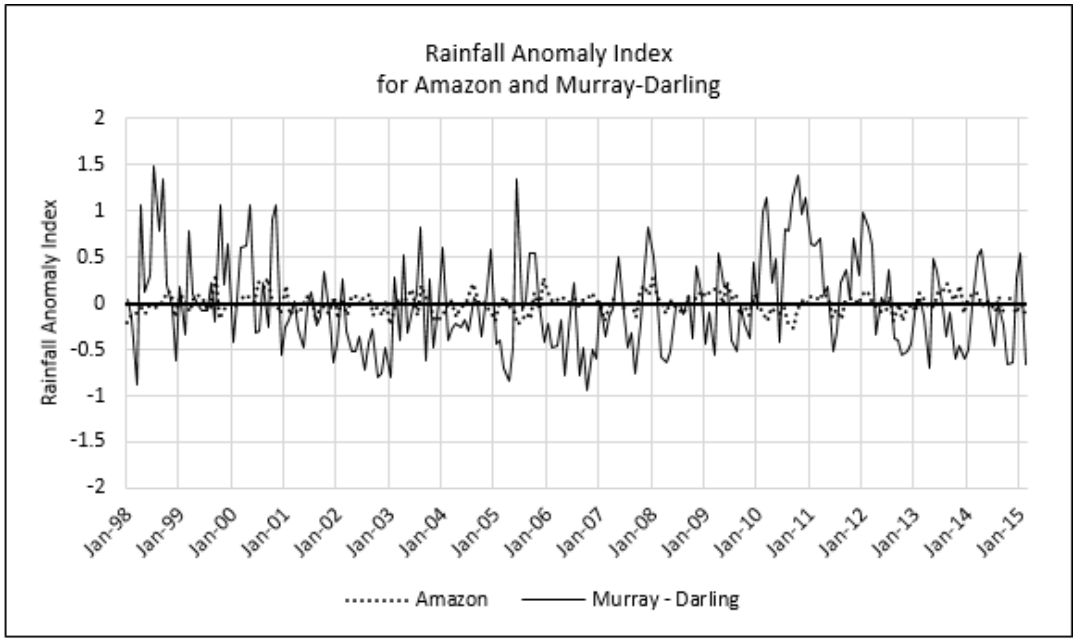

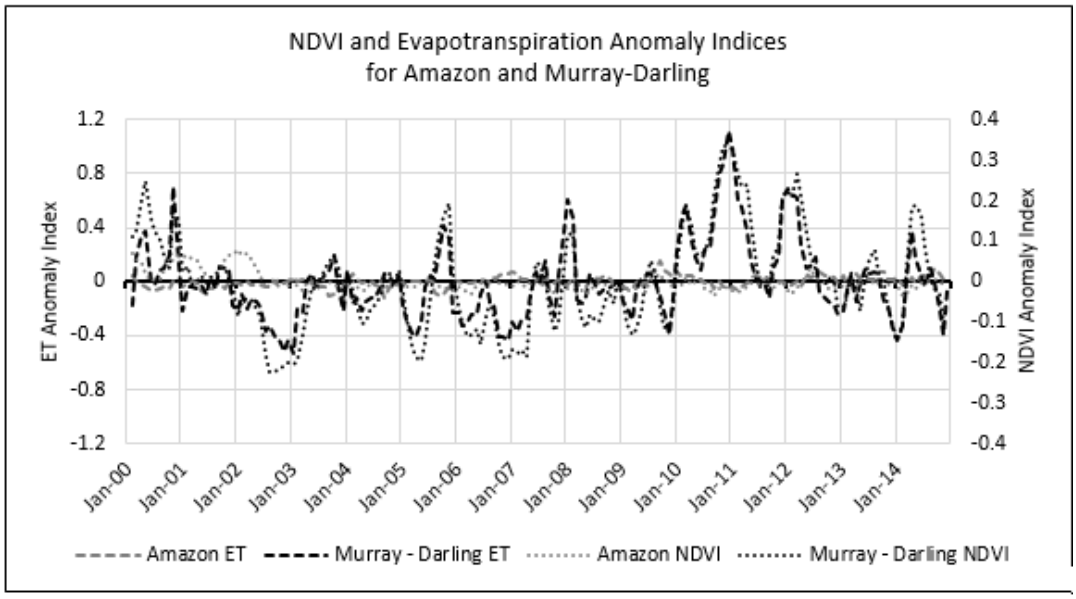

999
1000
1001
1002 Figure 9 Comparison for the Amazon River basin and the Murray-Darling basin (a)
1003 Monthly rainfall anomaly index and (b) Monthly NDVI and ET anomaly index
1004
1005
1006
1007
1008